NUCLEAR DATA AND MEASUREMENTS SERIES

ANL/NDM-115

Evaluated Neutronic File for Indium

by

A.B. Smith, S. Chiba, D.L. Smith, J.W. Meadows,
P.T. Guenther, R.D. Lawson, and R.J. Howerton

January 1990

ARGONNE NATIONAL LABORATORY,
ARGONNE, ILLINOIS 60439, U.S.A.

NUCLEAR DATA AND MEASUREMENTS SERIES

ANL/NDM-115

EVALUATED NEUTRONIC FILE FOR INDIUM

A. B. Smith, S. Chiba, D. L. Smith, J. W. Meadows,
P. T. Guenther, R. D. Lawson, and
R. J. Howerton

January 1990

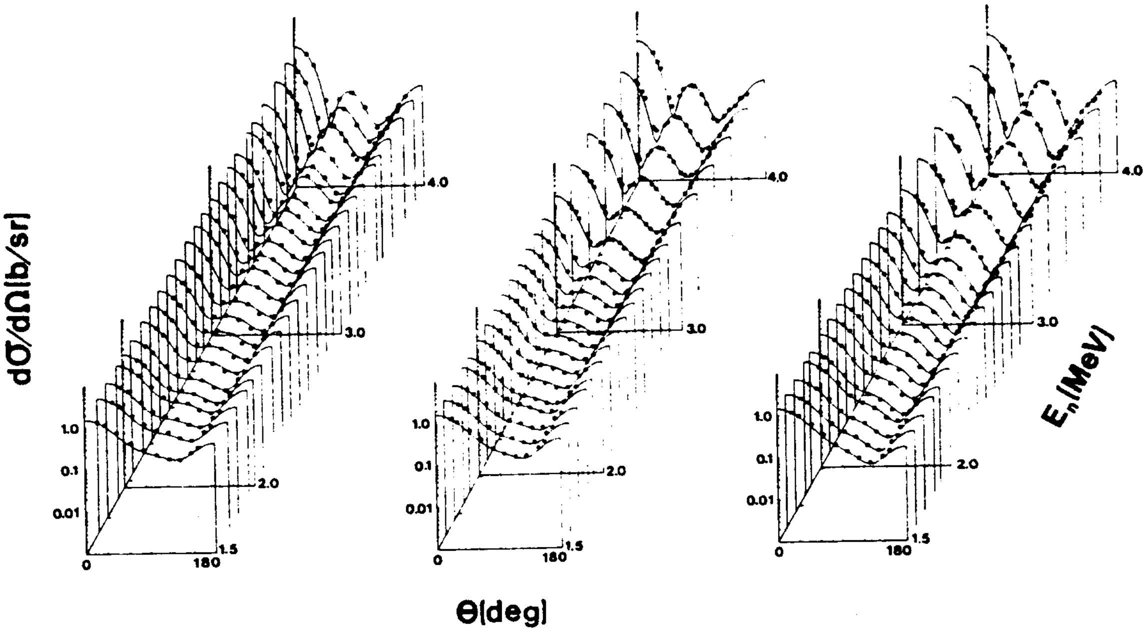

ARGONNE NATIONAL LABORATORY, ARGONNE, ILLINOIS

Operated by THE UNIVERSITY OF CHICAGO
for the U. S. DEPARTMENT OF ENERGY
under Contract W-31-109-Eng-38

Argonne National Laboratory, with facilities in the states of Illinois and Idaho, is owned by the United States government, and operated by The University of Chicago under the provisions of a contract with the Department of Energy.

This report has been reproduced from the best available copy.

Available from the
National Technical Information Service
U.S. Department of Commerce
5285 Port Royal Road
Springfield, VA 22161

Price: Printed Copy A03
Microfiche A01

ANL/NDM–115

EVALUATED NEUTRONIC FILE FOR INDIUM*

by

A. B. Smith, S. Chiba†, D. L. Smith, J. W. Meadows,
P. T. Guenther, and R. D. Lawson
ARGONNE NATIONAL LABORATORY

and

R. J. Howerton
LAWRENCE LIVERMORE NATIONAL LABORATORY

January 1990

Keywords

Neutronic evaluation for indium, 10^{-5} eV to 20 MeV.
Includes ^{115}In(n,n′)^{115m}In dosimetry evaluation.
ENDF/B–VI formats.

Engineering Physics Division
ARGONNE NATIONAL LABORATORY
9700 South Cass Avenue
Argonne, Illinois 60439
U.S.A.

*This work supported by the U.S. Department of Energy under Contract No. W–31–109–Eng–38.
†Visiting Scientist from Japan Atomic Energy Research Institute.

NUCLEAR DATA AND MEASUREMENTS SERIES

The Nuclear Data and Measurements Series presents results of studies in the field of microscopic nuclear data. The primary objective is the dissemination of information in the comprehensive form required for nuclear technology applications. This Series is devoted to: a) measured microscopic nuclear parameters, b) experimental techniques and facilities employed in measurements, c) the analysis, correlation and interpretation of nuclear data, and d) the evaluation of nuclear data. Contributions to this Series are reviewed to assure technical competence and, unless otherwise stated, the contents can be formally referenced. This Series does not supplant formal journal publication, but it does provide the more extensive information required for technological applications (e.g., tabulated numerical data) in a timely manner.

TABLE OF CONTENTS

INFORMATION ABOUT OTHER ISSUES OF THE ANL/NDM SERIES

A list of titles and authors for all the previous issues appears in each report of the series. The list for reports ANL/NDM–1 through ANL/NDM–75 appears in ANL/NDM–76, and ANL/NDM–91 contains the list for reports ANL/NDM–76 through ANL/NDM–90. Below is the list for ANL/NDM–91 up to the current report. Requests for a complete list of titles or for copies of previous reports should be directed to:

Section Secretary
Applied Nuclear Physics Section
Engineering Physics Division
Building 316
Argonne National Laboratory
9700 South Cass Avenue
Argonne, Illinois 60439
U.S.A.

ANL/NDM–91 A.B. Smith, P.T. Guenther and R.D. Lawson, *On the Energy Dependence of the Optical Model of Neutron Scattering from Niobium*, May 1985.

ANL/NDM–92 Donald L. Smith, *Nuclear Data Uncertainties (Vol.–I): Basic Concepts of Probability*, December 1988.

ANL/NDM–93 D.L. Smith, J.W. Meadows and M.M. Bretscher, *Integral Cross–section Measurements for* $^{7}Li(n,n't)^{4}He$, $^{27}Al(n,p)^{27}Mg$, $^{27}Al(n,\alpha)^{24}Na$, $^{58}Ni(n,p)^{58}Co$, *and* $^{60}Ni(n,p)^{60}Co$ *Relative to* ^{238}U *Neutron Fission in the Thick–target* $^{9}Be(d,n)^{10}B$ *Spectrum at* $E_d = 7$ *MeV*, October 1985.

ANL/NDM–94 A.B. Smith, D.L. Smith, P. Rousset, R.D. Lawson and R.J. Howerton, *Evaluated Neutronic Data File for Yttrium*, January 1986.

ANL/NDM–95 Donald L. Smith and James W. Meadows, *A Facility for High–intensity Neutron Irradiations Using Thick–target Sources at the Argonne Fast–neutron Generator*, May 1986.

ANL/NDM–96 M. Sugimoto, A.B. Smith and P.T. Guenther, *Ratio of the Prompt–fission–neutron Spectrum of Plutonium–239 to that of Uranium–235*, September 1986.

ANL/NDM–97 J.W. Meadows, *The Fission Cross Sections of* ^{230}Th, ^{232}Th, ^{233}U, ^{234}U, ^{236}U, ^{238}U, ^{237}Np, ^{239}Pu, *and* ^{242}Pu *Relative* ^{235}U *at 14.74 MeV Neutron Energy*, December 1986.

ANL/NDM–98 J.W. Meadows, *The Fission Cross Section Ratios and Error Analysis for Ten Thorium, Uranium, Neptunium and Plutonium Isotopes at 14.74–MeV Neutron Energy*, March 1987.

ANL/NDM–99 Donald L. Smith, *Some Comments on the Effects of Long–range Correlations in Covariance Matrices for Nuclear Data*, March 1987.

ANL/NDM–100 A.B. Smith, P.T. Guenther and R.D. Lawson, *The Energy Dependence of the Optical–model Potential for Fast–neutron Scattering from Bismuth*, May 1987.

ANL/NDM–101 A.B. Smith, P.T. Guenther, J.F. Whalen and R.D. Lawson, *Cobalt: Fast Neutrons and Physical Models*, July 1987.

ANL/NDM–102 D. L Smith, *Investigation of the Influence of the Neutron Spectrum in Determinations of Integral Neutron Cross–Section Ratios*, November 1987.

ANL/NDM–103 A.B. Smith, P.T. Guenther and B. Micklich, *Spectrum of Neutrons Emitted From a Thick Beryllium Target Bombarded With 7 MeV Deuterons*, January 1988.

ANL/NDM–104 L.P. Geraldo and D.L. Smith, *Some Thoughts on Positive Definiteness in the Consideration of Nuclear Data Covariance Matrices*, January 1988.

ANL/NDM–105 A.B. Smith, D.L. Smith, P.T. Guenther, J.W. Meadows, R.D. Lawson, R.J. Howerton, and T. Djemil, *Neutronic Evaluated Nuclear–Data File for Vanadium*, May 1988.

ANL/NDM–106 A.B. Smith, P.T. Guenther, and R.D. Lawson, *Fast–Neutron Elastic Scattering from Elemental Vanadium*, March 1988.

ANL/NDM–107 P. Guenther, R. Lawson, J. Meadows, M. Sugimoto, A. Smith, D. Smith, and R. Howerton, *An Evaluated Neutronic Data File for Elemental Cobalt*, August 1988.

ANL/NDM–108 M. Sugimoto, P.T. Guenther, J.E. Lynn, A.B. Smith, and J.F. Whalen, *Some Comments on the Interaction of Fast–Neutrons with Beryllium*, November 1988.

ANL/NDM–109 P.T. Guenther, R.D. Lawson, J.W. Meadows, A.B. Smith, D.L. Smith, and M. Sugimoto, *An Evaluated Neutronic Data File for Bismuth*, November 1989.

ANL/NDM–110 D.L. Smith and L.P. Geraldo, *A Vector Model for Error Propatation*, March 1989.

ANL/NDM–111 J.E. Lynn, *Fifty Years of Nuclear Fission*, June 1989.

ANL/NDM–112 S. Chiba, P.T. Guenther, and A.B. Smith, *Some Remarks on the Neutron Elastic– and Inelastic–Scattering Cross Sections of Palladium*, May 1989.

ANL/NDM–113 J.E. Lynn, *Resonance Effects in Neutron Scattering Lengths*, June 1989.

ANL/NDM–114 A.B. Smith, R.D. Lawson, and P.T. Guenther, *Ambiguities in the Elastic Scattering of 8 MeV Neutrons from Adjacent Nuclei*, October 1989.

EVALUATED NEUTRONIC FILE FOR INDIUM

A. B. Smith, S. Chiba, D. L. Smith, J. W. Meadows,
P. T. Guenther, R. D. Lawson, and R. J. Howerton

ABSTRACT

A comprehensive evaluated neutronic data file for elemental indium is documented. This file, extending from 10^{-5} eV to 20 MeV, is presented in the ENDF/B–VI format, and contains all neutron–induced processes necessary for the vast majority of neutronic applications. In addition, an evaluation of the ^{115}In(n,n′)^{115m}In dosimetry reaction is presented as a separate file. Attention is given in quantitative values, with corresponding uncertainty information. These files have been submitted for consideration as a part of the ENDF/B–VI national evaluated–file system.

I. INTRODUCTION

Indium has been used in nuclear applications (primarily as a dosimeter) for a half century; it is employed in superconductors, appears as a fission product, and has a large (n,2n′) cross section making it a good neutron multiplier. Despite these facts, the ENDF/B evaluated file system does not contain an elemental indium neutronic file. The element consists of the two isotopes ^{113}In (4.3%) and ^{115}In (95.7%), and the ENDF/B system[1] contains fission–product files for both. The latter are special purpose files, and completely devoid of important neutron–induced reactions, such as the large (n,2n′) processes.

In view of the above, the present evaluation was undertaken in order to provide a comprehensive elemental evaluated neutronic data file for indium. The file contains essentially all reactions of interest in neutronic applications, and it gives attention to uncertainty specification. In addition, the evaluation of the ^{115}In(n,n′)^{115m}In dosimetry reaction is specifically treated with the results given in a separate dosimetry file. However, there may remain additional special applications where these files are not sufficient. In those few cases, the user should refer to appropriate special–purpose files. The numerical files documented in this report have been transmitted to the National Nuclear Data Center for consideration as a part of ENDF/B–VI. Those interested in obtaining a copy of the numerical values should contact that Center, or the authors.

II. RESONANCE PARAMETERS

Resonance parameters appropriate to the two isotopes, ^{113,115}In, are used to describe the neutron interaction with indium up to 2 keV. The parameters are taken from the work of Mughabghab,[2] as modified by Mughabghab and Dunford for completeness, with small changes in the scattering radius to agree with experiment. The code RECENT[3] was used to calculate the cross sections from the parameters. At thermal energy, the neutron capture and elastic–scattering cross sections, and the infinitely–dilute resonance integral, agreed with the values of Ref. 2 within the stated uncertainties.

III. ENERGY–AVERAGED NEUTRON TOTAL CROSS SECTIONS

The evaluated energy–averaged total cross sections extend from the upper limit of the resonance representation (2 keV) to 20 MeV. The evaluation is based upon measured neutron total cross sections, as available from the National Nuclear Data Center.[4] The database consists of the 23 citations (Refs. 5–27). The average age of these data is about 25 years, with only four citations in the last decade. None of the data were obtained with the large white–source facilities. This is not a particularly good database from which to construct an evaluation.

The above database was inspected on large–scale plots. Some of the data sets were clearly inconsistent with the body of the information and were not used, as noted in the references. Since the objective was an energy–averaged behavior, the accepted data sets were averaged over 100 keV intervals to 1 MeV, over 200 keV intervals from 1–2 MeV, over 300 keV intervals from 2–4 MeV, over 400 keV from 4–6 MeV, and over 500 keV intervals at energies above 6 MeV. These averaging intervals preserved the general slow energy dependence of the cross section, smoothed statistical fluctuations, and reduced the number of data points to more manageable proportions. The averaging procedure preserved the uncertainties assigned by the various authors, assuming that they were of a statistical nature. The resulting energy–averaged database was reasonably consistent from data set to data set, but there clearly were systematic differences of a few percent. A definite statement of systematic uncertainty was not available for any of the data; thus, subjective estimates had to be made. With no specific information to guide the choice, they were only crude, varying from ≈ 2% to 5% or more, depending on what appeared to be the quality and scope of the data in the individual sets. These systematic uncertainty estimates appeared to be relatively consistent with the differences evident between the various data sets. The effects of the subjective judgments were unavoidably propagated through the evaluation procedure. There is no alternative until such time as a far better database is available, with explicit statement of systematic uncertainties. The statistical and systematic uncertainties were combined to obtain the total uncertainties of the energy–averaged data values. At low energies, the total cross sections may be distorted by self–shielding effects. This was ignored, as the experimental information did not make possible an assessment of such effects, or, if present, their correction. The resulting energy–averaged database, with its uncertainties, is shown in Fig. 1

The preceding energy–averaged database was evaluated using the statistical procedure of the computer code GMA.[28] The procedure used an energy mesh that was sufficiently fine to assure good representation of the energy dependence of the cross section. The GMA results will fluctuate, following small artifacts of the underlying data. These fluctuations have no physical meaning, and they were smoothed by chi–square fitting the GMA results with a conventional spherical optical model, concurrently varying the ten parameters, real and imaginary potential strengths (each having a quadratic energy dependence), radii, and diffusenesses. The resulting model parameters were reasonable, but were used only to provide a physically rational smoothing of the GMA results. The resulting evaluated cross sections compare very favorably with the input database, as shown in Fig. 1.

The GMA procedure provides a measure of uncertainty and the associated covariance matrix. Characteristically, the uncertainties are smaller than one would subjectively estimate from the database. Therefore, the GMA uncertainties were increased by a factor of two for this file. These adjusted uncertainty quantities are set forth in Table 1. An impression of the covariance matrix is given in the three–dimensional illustration of Fig. 2. The user is cautioned that this uncertainty information provides only qualitative guidance, and that it is, to a considerable extent, a reflection of the above–cited subjective judgments of systematic uncertainties. However, the values of Table 1 are reasonably consistent with the comparisons of measured and evaluated cross sections shown in Fig. 1.

Fig. 1 also compares the present evaluation with that given in ENDF/B–V. The ENDF/B–V file gives the two indium isotopic cross sections (^{113}In and ^{115}In), so they were combined to yield the elemental ENDF/B–V cross section shown in Fig. 1. The two elemental evaluations differ by ≈ 10% or more over large energy ranges. These are considerable differences which will be propagated, and magnified, in other portions of the file. In order to significantly improve the present evaluation, some comprehensive new

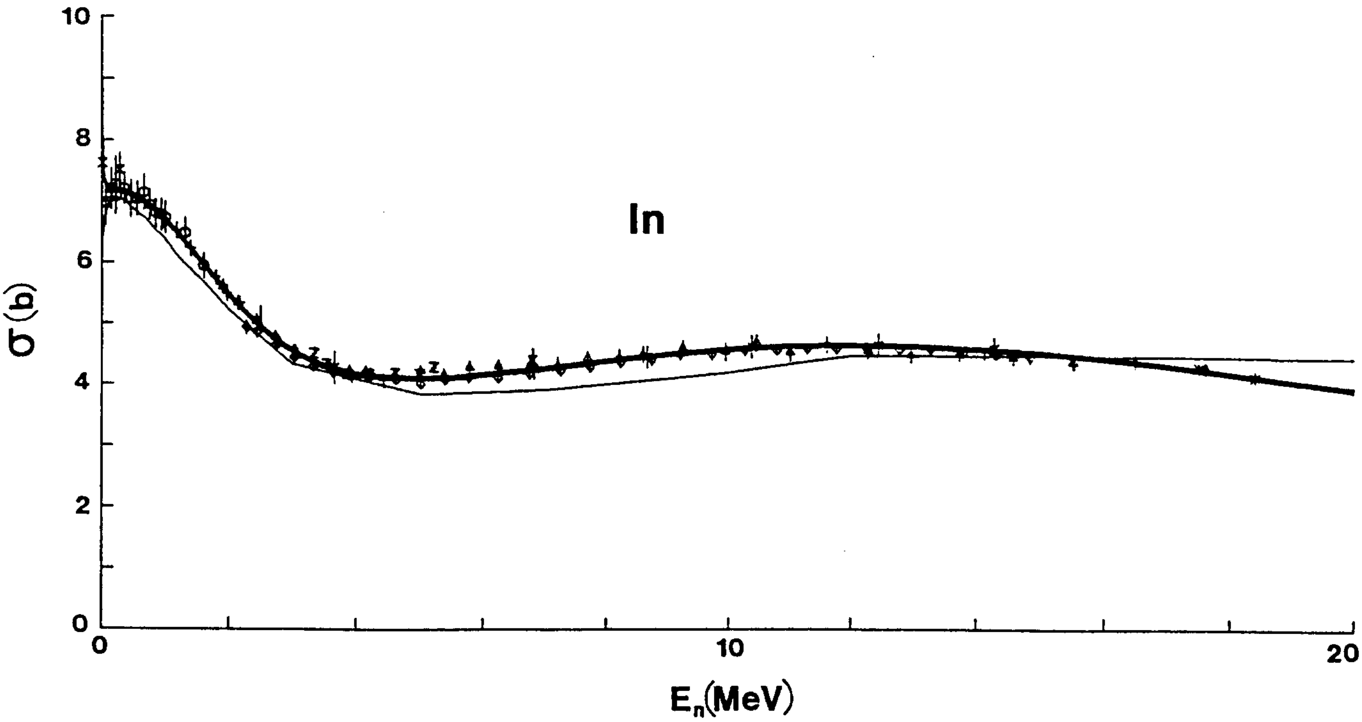

Fig. 1. Energy–averaged neutron total cross sections of elemental indium. The various data symbols indicate the experimental energy–averaged cross–section values used in the evaluation, together with their respective uncertainties. The heavy curve indicates the result of the present evaluation, and the light curve the evaluation given in ENDF/B–V.

Table 1

Evaluated total–cross–section uncertainties

E_n(MeV)	Uncertainty(%)
0.25	3.14
0.50	4.71
0.75	2.56
1.0	2.09
1.25	2.03
1.50	1.84
2.00	1.62
2.50	1.55
3.00	1.59
3.50	1.53
4.00	1.52
4.50	1.55
5.00	1.53
6.00	1.57
7.00	1.58
8.00	1.64
9.00	1.64
10.00	1.59
11.00	1.56
12.00	1.52
13.00	1.53
14.00	1.54
15.00	1.74
16.00	3.55
17.00	3.57
18.00	2.82
20.00	4.00

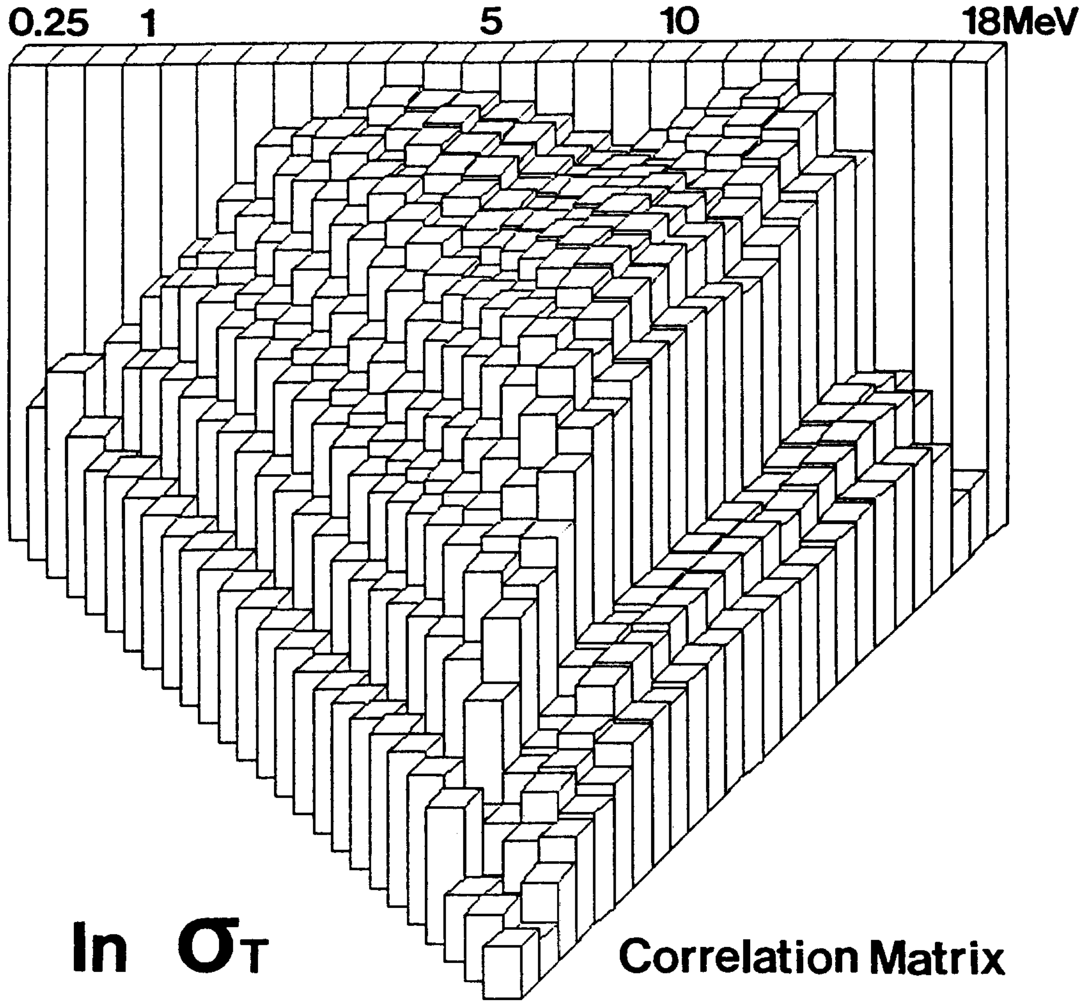

Fig. 2. A three–dimensional illustration of the covariance matrix for the evaluated neutron total cross sections of indium.

total–cross–section measurements are required. These should address, particularly, the energy ranges 1 keV to 1 MeV and 14 to 20 MeV.

IV. ENERGY–AVERAGED NEUTRON ELASTIC–SCATTERING CROSS SECTIONS

The energy–averaged neutron elastic–scattering cross sections extend from 2 keV (the upper limit of the resonance region) to 20 MeV. Up to 15 MeV they are based upon the detailed study of measured differential elastic–scattering cross sections described in Refs. 29 and 30. Above 15 MeV the model of Ref. 30 was used to extrapolate to 20 MeV, as there is no experimental information available. The extrapolation is believed to be reasonably reliable, since the model gives a very good description of both the total neutron cross section to 20 MeV and the observed differential elastic scattering below ≈ 15 MeV, as discussed in Ref. 30. The resulting evaluated elastic–scattering cross sections are compared with those given in ENDF/B–V in Fig. 3. There are differences between the two evaluations over wide energy ranges, approaching approximately a factor of two at 20 MeV. These differences, together with the differences in the above evaluated total cross sections, imply large differences in the nonelastic cross sections of the two files that will impact on other aspects of the evaluations.

The relative evaluated angle–differential elastic–scattering distributions are expressed in the form of F_ℓ coefficients, and illustrated in Fig. 4. They give considerably more detail than is available from ENDF/B–V. These relative distributions, together with the corresponding angle–integrated cross sections, are consistent with Wick's Limit[31] as determined from the evaluated neutron total cross section. Final small adjustments in the elastic–scattering cross section were made to assure that the neutron total cross section is exactly the sum of the partial cross sections.

The uncertainties associated with the above evaluated angle–integrated elastic-scattering cross section are estimated to be ≈ <5% to 10 MeV, increasing to ≈ 10% at 20 MeV in approximately a linear manner.

The experimental database and models upon which this elastic–scattering evaluation is based are quite comprehensive up to at least 10 MeV. There is a less detailed distribution at ≈ 15 MeV, but nothing at higher energies. The extrapolation to these higher energies is believed to be reasonably reliable, but one would have more confidence if there were several detailed differential measurements between 10 and 20 MeV. To be useful, they would have to have overall uncertainties of ≈ <5% in regions of appreciable cross section, and span the angular range ≈ 10° to 160° in $5^\circ - 10^\circ$ steps. Such measurements are feasible, but not simple.

V. INELASTIC NEUTRON–SCATTERING PROCESSES

A. Discrete Inelastic Excitations

Primary attention was given to the inelastic–neutron excitation of discrete levels in the prominent isotope, ^{115}In (95.7% abundant). These have been carefully studied in a

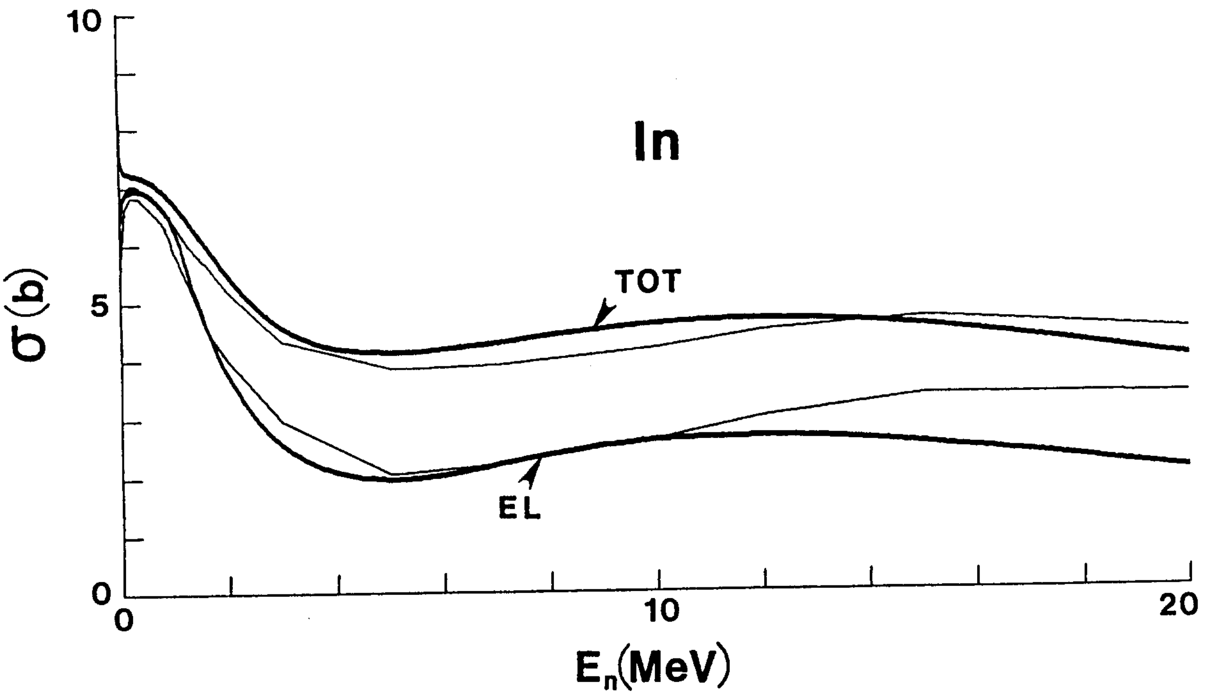

Fig. 3. The present indium evaluated neutron total and elastic–scattering cross sections (heavy curves) compared with the corresponding values of ENDF/B–V (light curves).

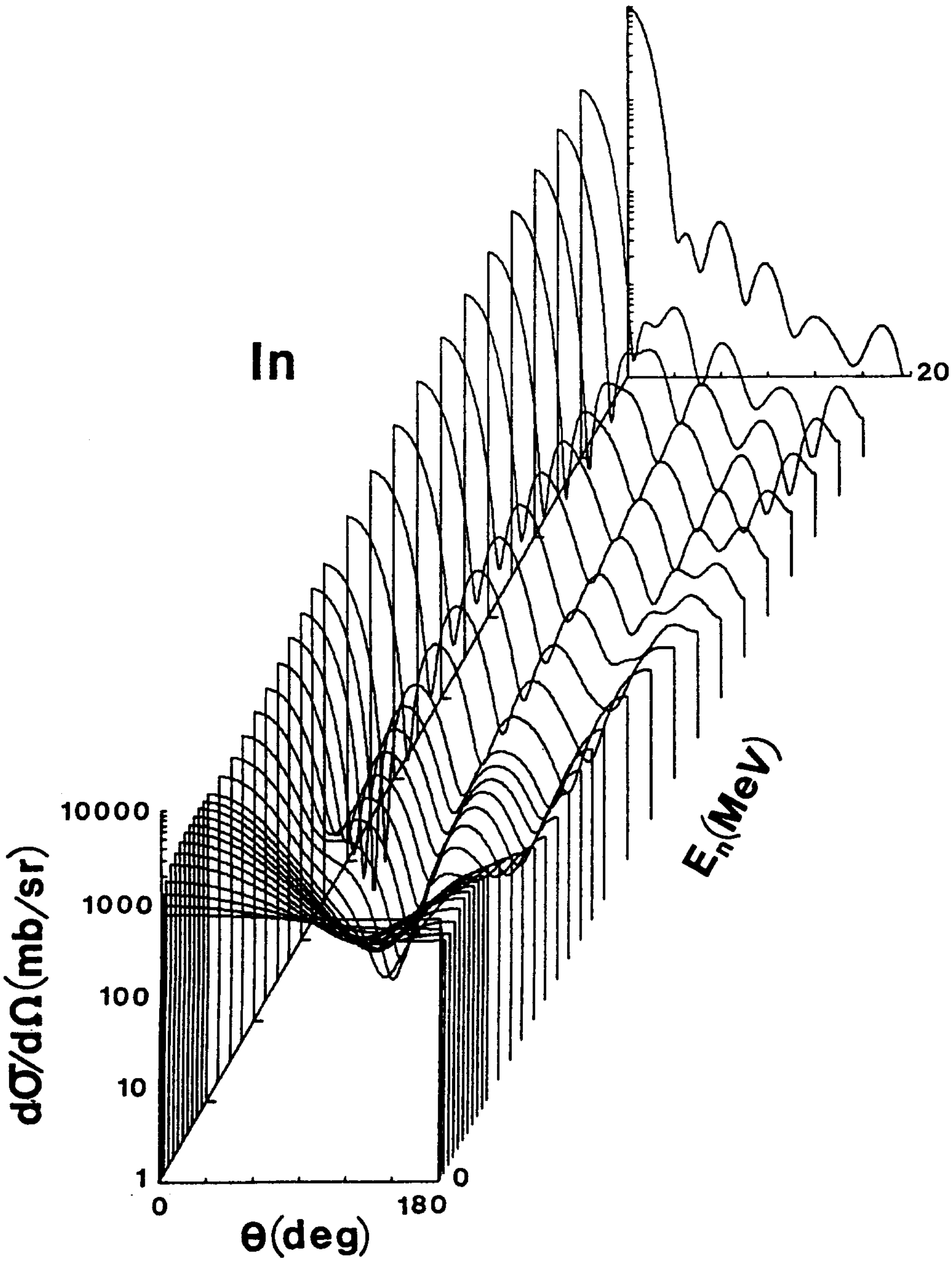

Fig. 4. Relative angle–differential elastic–scattering cross sections of indium from the present evaluation. The cross sections are presented in the laboratory coordinate system.

cooperative experimental program between this Laboratory and the National Accelerator Laboratory (Faure, South Africa).[29] From that work an optical–statistical model was derived that gave a good quantitative description of the observed inelastic–scattering cross sections within several MeV of the respective thresholds. That low–energy model reasonably matches the higher–energy model of Ref. 30 at an energy of several MeV. For the present evaluation, sixteen ^{115}In levels were considered up to excitations of ≈ 1.5 MeV, with the excitation energies and J^{π} values taken from Ref. 29. The corresponding inelastic–scattering cross sections were calculated using the optical–statistical model,[30] with results essentially identical to those given in Ref. 29. They are supported by the experimental results of Ref. 29. The calculations used the statistical representation of Gilbert and Cameron[32] to determine channel competition at higher energies. The same calculations give a good representation of the neutron total and elastic–scattering cross sections, as discussed in Ref. 30. For completeness, the same method was used to determine the discrete inelastic–scattering cross sections of the minor ^{113}In isotope (4.3% abundant). In the latter case, twelve excited levels below an energy of ≈ 1.5 MeV were used, with the excitations and J^{π} values of Ref. 33. Thus, in total, the evaluation contains 28 discrete neutron inelastic–scattering groups, with excitations up to ≈ 1.5 MeV. Their cumulative sum is shown by the "B" curve of Fig. 5. The angular distributions of the scattered neutrons were assumed to be isotropic in all cases. This is a reasonable assumption, as the processes are due to compound–nucleus reactions which are symmetric in angle about 90°, and, in all cases, do not significantly deviate from isotropy. The estimated uncertainty associated with the cumulative sum of these discrete inelastic-scattering cross sections is ≈ 5% over energy regions where the sum of the cross sections is of appreciable magnitude. The uncertainties associated with the individual inelastic cross sections, particularly where the cross sections are small, may be much larger.

B. Continuum Inelastic Scattering

Above incident energies of ≈ 1.5 MeV, the continuum inelastic–scattering cross section rises rapidly to large values, exceeding 2 b. The evaluation determines the continuum inelastic–scattering cross section from the difference between the nonelastic cross section and the other partial cross sections. Over much of the energy range, the evaluated neutron total and elastic–scattering cross sections determine the nonelastic cross section to ≈ 5%. Below 10 MeV, the major contribution is from the inelastic–scattering cross section. Above ≈ 10 MeV, the (n,2n′) cross section rises rapidly to relatively large values, with a complementary sharp decrease in the continuum inelastic scattering cross section (which falls to an ≈ 200 mb level at 20 MeV) determined by pre–compound inelastic–scattering processes. Above ≈ 16 MeV the (n,3n′) cross section also becomes a factor. These general energy–dependent trends are illustrated in Fig. 5. The uncertainties associated with the total inelastic–scattering cross section are estimated to be ≈ 5% from 1 to 10 MeV. They are larger (10%) below 1 MeV, and approximately the same size above 10 MeV.

The inelastic–scattering cross sections of the present evaluation are grossly different from those given in ENDF/B–V, as illustrated in Fig. 5. Below ≈ 10 MeV the inelastic-scattering cross sections of the two evaluations differ by ≈ 20%. At higher energies the differences are even larger, amounting to ≈ 500% at 20 MeV. Clearly, above ≈ 1.5 MeV the inelastic–scattering cross sections of ENDF/B–V have a physically unrealistic shape. Thus, the ENDF/B–V isotopic indium evaluations should not be used for general–purpose neutronic calculations, particularly where the application is sensitive to higher–energy neutron–induced processes.

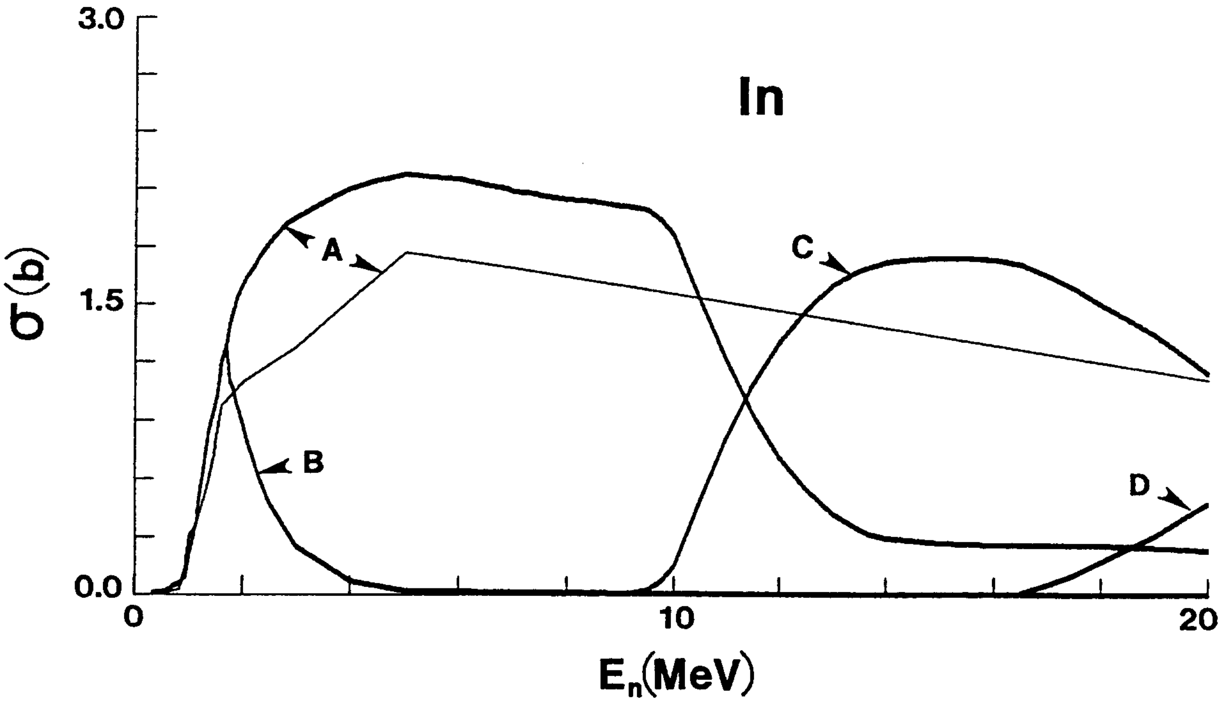

Fig. 5. Evaluated (n,n′), (n,2n′) and (n,3n′) cross sections. The present evaluation is indicated by heavy curves, while that of ENDF/B–V by light curves. Letters denote the contributing processes as: "A" = total inelastic–scattering cross section, "B" = sum of discrete inelastic–scattering cross sections, "C" = the (n,2n′) cross section, and "D" = the (n,3n′) cross section.

The continuum neutron spectra emitted as a result of inelastic–scattering processes were estimated using direct experimental measurements[34] below $\approx$ 8 MeV. They were extrapolated to higher energies using model calculations, as described below. These considerations included contributions from pre–compound processes at energies above $\approx$ 8 MeV. The evaluation assumes that the neutron emission from the continuum processes is isotropic. This simplifying assumption does not properly represent the forward–angle bias of the pre–compound emission processes, but it makes the evaluation suitable for the large majority of processing codes that do not treat angle–energy correlations. Inclusion of the additional complexity of energy–angle correlations will not generally enhance the applications potential in most cases, as the observed emitted spectra are essentially isotropic below $\approx$ 8 MeV.[34]

The angle and energy distribution of the continuum spectrum of emitted neutrons with energies of $\lesssim$ 8 MeV was determined from comprehensive experimental measurements[34] at this laboratory. Above 8 MeV the evaluation is based upon calculated quantities.

The experimental neutron emission data used below 8 MeV were measured at ten angles distributed between 30° and 160°. The detectors were biased so as to reliably observe neutrons with energies exceeding $\approx$ 1 MeV. The principal neutron–emission information provided by these measurements is summarized as follows. For excitation energies exceeding a few MeV, the angular distributions in the center–of–mass are essentially isotropic. The corresponding neutron–emission spectra are reasonably described by

$$N(E_n) = E_n \cdot \exp(-E_n/T),$$

where T is the nuclear temperature at the given incident–neutron energy. This expression is used to extrapolate the experimental results to lower energies, below the detector cut–off. At the highest emission energies, there is evidence for both pre–compound and direct processes, as the emission spectra are harder than a single–component evaporation formalism would predict, and the corresponding angular distributions evince modest forward peaking.

The methodology of the experimental measurements and their analysis are treated in detail in Ref. 34. Here we only outline those procedures required to construct the relevant entries for the file. First, the ratios of time–of–flight neutron spectra resulting from the bombardment of indium and from the spontaneous fission of ^{252}Cf were constructed and summed into 200 keV wide Q–value bins. These laboratory distributions were corrected for finite–sample effects and then angle integrated. The resultant energy–differential ratios, R, were fitted in the center–of–mass system with the linear expression

$$\ln(R) - 0.5 \cdot \ln(E_n) = -E_n(1/T_{In} - 1/T_{Cf}),$$

from which T_{In} could be deduced assuming T_{Cf} = 1.42 MeV. The same angle–integrated Q–value bins were also multiplied by corresponding segments of the Maxwellian for the ^{252}Cf fission–neutron spectrum to obtain the relative cross sections. The evaporation spectrum was then matched to these cross sections over the same emission–neutron energy range used in the fit. Finally, this composite was transformed back into the laboratory system. This process was repeated at each incident–neutron energy.

Above 8 MeV the calculated continuum–emission spectra are made up of contributions from the (n,n′), (n,2n′), (n,3n′), (n;p,n′) and (n;α,n′) reactions. The (n;n′,p) and (n;n′α) reactions were not included in the present evaluation. Model calculations indicate that these two latter branches account for less than 10% of the respective total reactions, and for only ≈ 1% of the total neutron emission.

The individual spectra were calculated using the computer codes ALICE[35] and CADE.[36] ALICE calculates cross sections and emission spectra using the hybrid model for pre–compound processes and the Weisskopf–Ewing evaporation model for compound decay. For simplicity, in the present calculations it was assumed that the pre–compound processes only involve the emission of a single nucleon. This is a reasonable assumption up to 20 MeV where multi–particle pre–compound processes are still only a few percent of the total reaction cross section. CADE carries out compound–nucleus calculations using the Weisskopf–Ewing method and the level–density formalism of Brancazio and Cameron.[37] γ–ray emission is described by the giant–dipole formalism. This program was used to divide the spectrum of the first emitted neutron among the various reactions. This can also be done with ALICE, but it was desirable to include the effect of the (n;n′,γ) channel for excitation energies above the (n,2n′) threshold, and ALICE has no convenient γ–ray channel.

The parameters of ALICE were adjusted at each energy so that the ratios (n,n′)/(n,2n′) and (n,3n′)/(n,2n′) agreed with the values obtained in the evaluation; then the neutron spectra associated with each component of the individual reactions were calculated using the methods described in Ref. 38. These results were then transformed to the laboratory coordinate system, maintaining energy correlation but assuming no angle correlation. When these components are combined, neutron spectra are obtained which are qualitatively consistent with those observed for other similar materials. There are some artifacts in the calculated emission spectra due to the rather coarse energy mesh used, and to the non–exact matching of various components near reaction thresholds. However, the initial adjustment of ALICE parameters, noted above, kept these artifacts small.

VI. NEUTRON RADIATIVE–CAPTURE CROSS SECTIONS

The database consisted of measured values available from the files of the National Nuclear Data Center. These data were primarily obtained using prompt–detection techniques, with some activation results. The data above 2 keV are cited in Refs. 39–52. These data were plotted on a large scale, and carefully inspected. An illustrative plot is shown in Fig. 6. It was evident that: i) the data scatter by significant amounts, ii) the majority of the data are at energies of < ≈ 100 keV, iii) there is only one questionable measurement above ≈ 5 MeV, and iv) the cross section is relatively large (i.e., > 200 mb) up to more than an MeV. The measurements were made relative to a variety of reference standards that have changed over the intervening years. However, these changes are relatively small compared to the discrepancies between the measured values, and thus no effort was made to correct the measured results to ENDF/B–VI standards, as the task would be tedious and would not substantively improve the database.

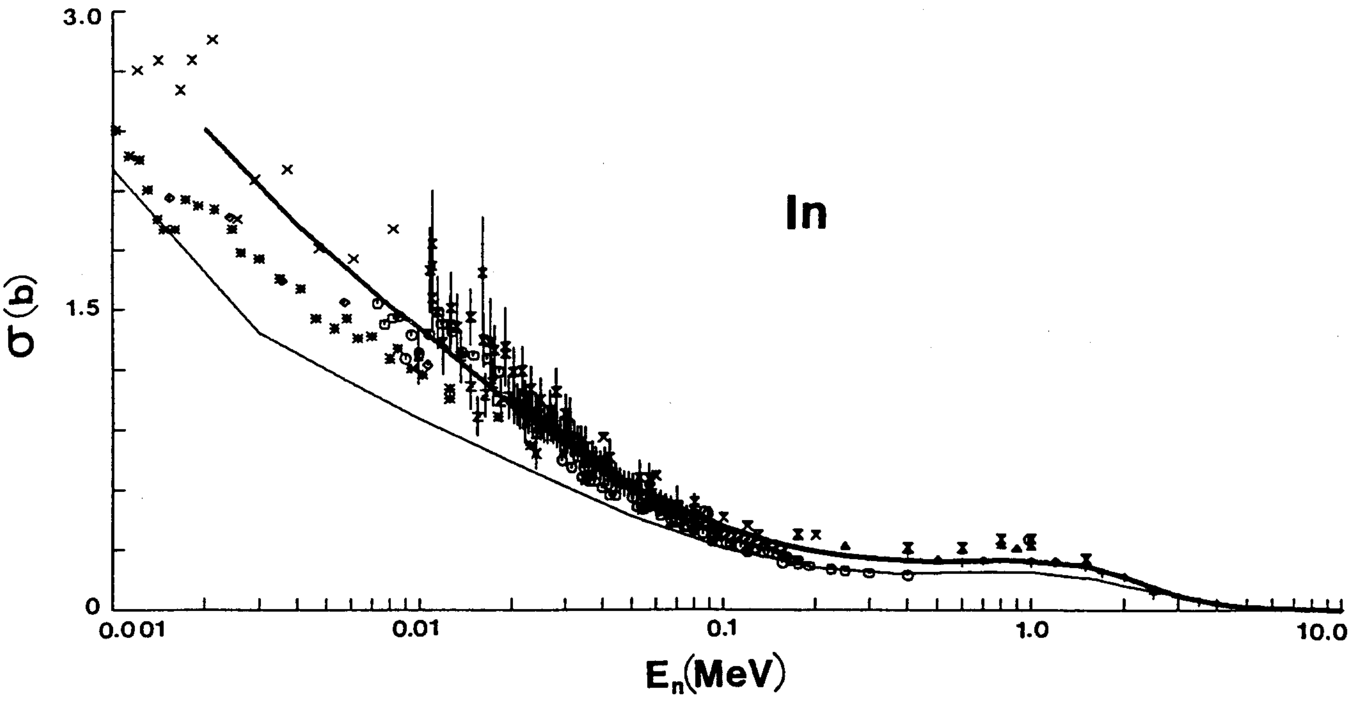

Fig. 6. Neutron radiative–capture cross sections of indium. The experimental results are indicated by symbols. The heavy curve denotes the present evaluation, and the light curve that of ENDF/B–V.

In view of the above discrepant data, the evaluation is based upon a simple giant–dipole–resonance calculation, employing the model of Ref. 53, with the S_0 strength function adjusted to obtain what was subjectively judged to be a "best" description of the measured values. The result is compared with the measured data in Fig. 6. This method properly accounts for channel competition from the inelastic–scattering processes. In view of the poor quality of the database, the estimated uncertainties associated with this evaluation are quite large; ≈ 10% – 15% to 100 keV, 15% – 25% from 100 keV to 2 MeV, and even larger at higher energies where few reliable data are available. These are very large uncertainties in a capture cross section that is not small below several MeV.

Figure 6 also compares the present evaluation with that given in ENDF/B–V. The ENDF/B–V values are generally much smaller than those of the present evaluation (i.e., by 35–40% at 10 keV, ≈ 35% at 50 keV, ≈ 25% at 100 keV, and by ≈ 40% in the 0.5 to 1 MeV range). Only one data set supports the ENDF/B–V evaluation, and then only over a very limited energy range. This is remarkable, considering the fact that most of the experimental data pre–dates ENDF/B–V by a number of years. These are large differences, considerably exceeding the respective uncertainties associated with the present evaluation.

It will be difficult to improve the present evaluation without detailed new measurements over the entire energy range. The cross section is large and can be obtained by means of relatively straightforward measurements.

VII. (n,2n′) AND (n,3n′) PROCESSES

Experimental knowledge of the (n,2n′) cross sections of indium is based entirely on the results of activation measurements. There are no experimental results obtained using direct–neutron–detection methods. For both the indium isotopes, the primary activity resulting from the (n,2n′) process is due to the decay of a metastable state. The interaction with the primary isotope, ^{115}In, results in a metastable state (5^+, 190 keV) in ^{114}In which decays with a 49.5 d half–life by means of an E4 transition to the ground state (1^+), which has a half–life of 71.9 s.[33] The (n,2n′) process also directly populates the ground state. The interaction with the minor isotope, ^{113}In, is analogous, primarily populating the metastable state (4^+, 155 keV) in ^{112}In which decays with a 20.9 min half-life to the ground state (1^+) which, in turn, decays with a 14.4 min half–life.[33] The ^{115}In(n,2n′)^{114m} reaction has been extensively studied, and there have been some measurements of the ^{115}In(n,2n′)^{114g}In cross sections, primarily near an incident energy of 14 MeV. In addition, there have been several measurements of the isomer ratio near 14 MeV. The experimental determination of cross sections for the ^{113}In(n,2n′)^{112m}In and ^{113}In(n,2n′)^{112g}In processes is much less comprehensive, and largely confined to incident energies of ≈ 14 MeV. The experimental results are given in Refs. 54–78.

The evaluation is primarily based upon the experimental data for the ^{115}In(n,2n′) processes, supported by statistical model calculations using the computer code CADE.[36] That code does not include pre–compound contributions, but they are relatively small in regions where the cross section is large. The experimental database for the ^{115}In(n,2n′)^{114m}In reaction is shown in Fig. 7. The experimental data are reasonably consistent, except for three data sets, each spanning the relatively large energy range from ≈ 13 to 17 MeV. Each of the discrepant sets has lower cross sections than the body of the

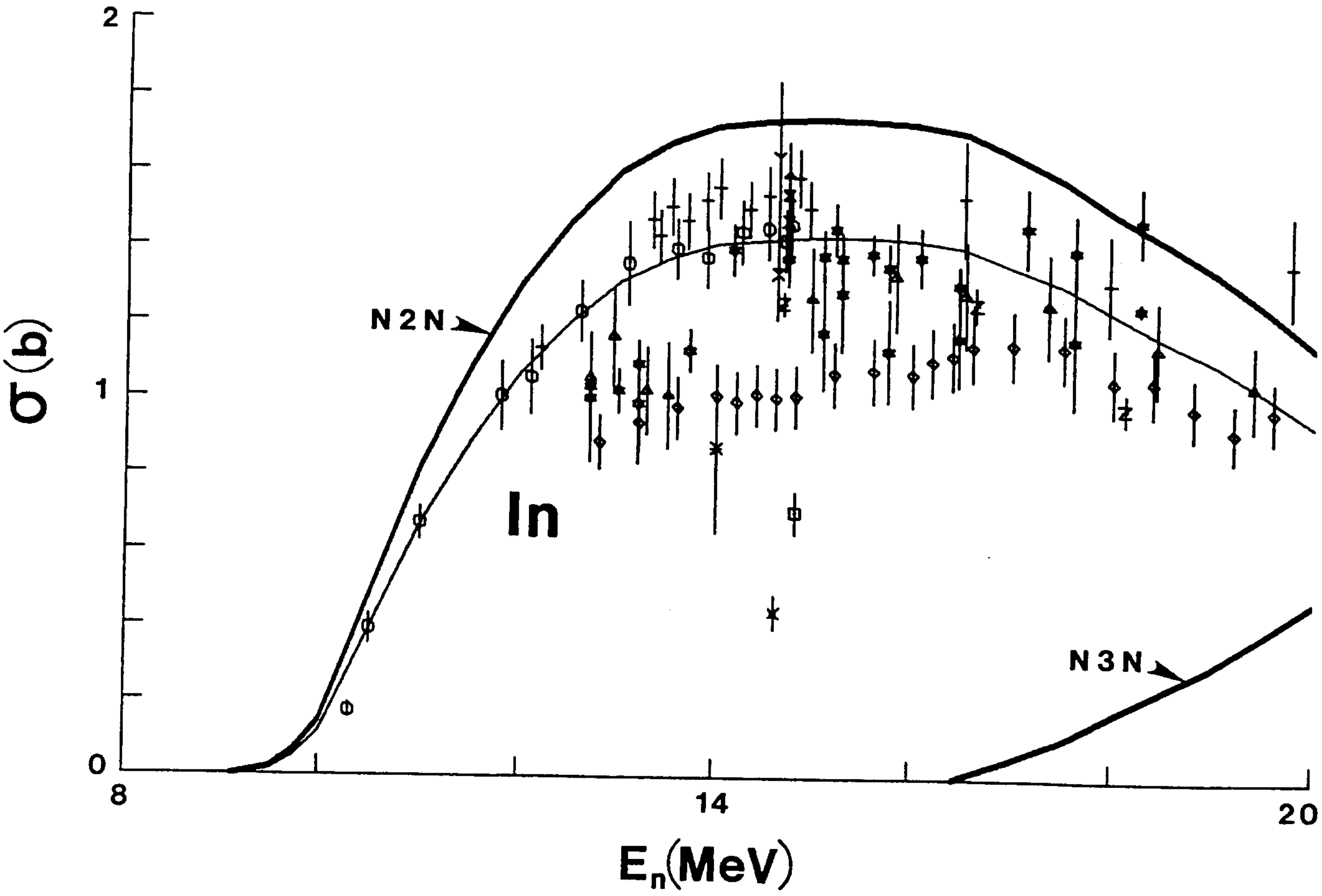

Fig. 7. (n,2n′) and (n,3n′) cross sections of indium. Measured values of the ^{115}In(n,2n′)^{114m}In cross section (symbols) and the corresponding evaluation (light curve) are shown. The evaluated elemental (n,2n′) and (n,3n′) cross sections are indicated by the heavy curves.

information over much of the energy range, and an unusual energy–dependent shape that is not consistent with the calculational estimates, or with what one would expect physically. Therefore, these three data sets were abandoned. The evaluated ^{115}In(n,2n′)^{114m}In cross section was subjectively constructed from the database, with the result indicated in Fig. 7. The experimental results reasonably define the evaluation up to an incident energy of ≈ 16.5 MeV, where the (n,3n′) process sets in. At higher energies, the experimental values scatter, and the (n,3n′) cross section is uncertain, as discussed below.

The isomer activation ratio, m/g, determined either from separate measurements or direct ratio measurements, is ≈ 4.5 (± ≈ 15%) near an incident energy of 14 MeV. It was assumed that this ratio was constant throughout the energy range of the evaluation. That is probably a reasonable assumption, possibly excepting the threshold region where the cross sections are small. Using this isomer ratio, the evaluated ^{115}In(n,2n′) cross sections were constructed from the above ^{115}In(n,2n′)^{114m}In evaluated cross sections. The result is not particularly sensitive to the m/g isomer ratio, as it is certainly quite large.

The experiments define the ^{113}In(n,2n′)^{112g}In and ^{113}In(n,2n′)^{112m}In cross sections, and the respective m/g ratio, only near 14 MeV. However, the values are very similar to those obtained for the comparable ^{115}In(n,2n′)^{114}In processes. In view of this fact, and the small 4.3% abundance of ^{113}In in the elemental indium, the evaluation assumes that the ^{115}In(n,2n′) cross sections are equivalent to those of the element, and they have a slightly lower (≈ 0.8 MeV) threshold than the ^{113}In(n,2n′) reaction. The resulting elemental (n,2n′) cross section is shown in Fig. 7. It is large, approaching 2 b at the maximum. The energy–dependent shape is relatively consistent with the calculational prediction of the code CADE, and the difference between evaluated and calculated magnitudes is $\lesssim$ 10% up to the (n,3n′) threshold. The estimated uncertainties of the evaluation are: $\gtrsim$ 20% below 11 MeV, ≈ 10% from 11 to 13 MeV, 8% to 10% from 13 to 17 MeV, and up to ≈ 20% or more above 17 MeV. It is impossible to compare the present evaluation with the two ENDF/B–V isotopic indium files, as the latter do not contain either the (n,2n′) or (n,3n′) reactions.

The spectra of neutrons emitted through the (n,2n′) process were calculated using the computer codes CADE[36] and ALICE,[35] in conjunction with the calculation of inelastic–emission spectra cited in Sec. V. The neutron emission is assumed to be isotropic in the laboratory coordinate system. The calculated spectra (and the evaluation) are probably no more than qualitative.

Apparently, only one measurement of the In(n,3n′) cross section has been reported.[79] It involves only the 2.8 d activity resulting from the reaction ^{113}In(n,3n′)^{111}In. The corresponding cross–section values are quite small, 57 mb at 19.5 MeV, but rapidly increasing with energy (adjusted to the more recent branching–ratio values,[33] the measured cross section at 19.5 MeV is ≈ 60 mb). A reasonable extrapolation of these measured values gives an ^{113}In cross section of ≈ 120 mb at 20 MeV. The ^{115}In(n,3n′) threshold is ≈ 0.81 MeV lower than that of the ^{113}In(n,3n′) reaction, and thus, due to the rapid increase of the cross section with energy, it is reasonable to expect the ^{115}In(n,3n′) cross section to be 400–500 mb at 20 MeV. Calculations using ALICE[35] and CADE[36] predict somewhat larger cross sections than suggested by the above experimental evidence. The energy-dependent shape of the (n,2n′) cross section above the (n,3n′) threshold suggests a (n,3n′) cross section at 20 MeV of perhaps half a barn. The evaluated (n,3n′) cross sections, shown in Fig. 7, are based upon the the difference between the experimentally based (n,2n′) cross section and the general energy–dependent trend of the reaction cross section.

They are somewhat larger than suggested by the above experimental evidence, but less than the prediction of calculations. In view of the poor experimental situation above the (n,3n′) threshold, there are large uncertainties in the evaluated (n,3n′) cross sections (perhaps as much as 50%), but for most applications that is of little concern, as the (n,3n′) threshold is at a relatively high energy (≈ 16.5 MeV). The corresponding (n,3n′) emission spectra were estimated from the calculations cited in Sec. V, with results that are no more than qualitative. The ENDF/B–V files contain no (n,3n′) cross sections.

There would be more confidence in the evaluation if there were several (n,2n′) and (n,3n′) measurements using direct neutron–detection methods, thereby avoiding uncertainties associated with isomer ratios and decay schemes. Such measurements are not simple, but can be done with well–known techniques.

VIII. CHARGED–PARTICLE EMITTING PROCESSES

A number of reaction channels of this type are open below 20 MeV for both of the indium isotopes. The corresponding processes generally have very small cross sections, which are not well known. In the present evaluation, only the following ten interactions with the prominent isotope, ^{115}In, are considered.

Reaction	Q–value (MeV)
(n,p)	–0.666
(n;n′,p)	–6.811
(n,d)	–4.587
(n;n′.d)	–13.627
(n,t)	–7.370
(n;n,t)	–13.914
(n,^{3}He)	–9.362
(n;n′,^{3}He)	–17.853
(n,α)	+2.726
(n;n′,α)	–3.740

The respective Q–values are taken from the tabulation of Ref. 80. Analogous interactions with the minor isotope, ^{113}In, were ignored, as were some additional minor reactions with ^{115}In having cross sections well down into the micro–barn level (e.g., the (n,2p) process). All of the energetically allowed processes were calculated using the statistical code CADE,[36] with the addition of a pre–compound component determined using the code ALICE,[35] as described in Sec. V. The calculated results were then compared with available experimental information and the calculations adjusted, where judged appropriate, to obtain the evaluated quantities. The experimental database is very weak, and there are concerns about the quantitative predictions of the models. Thus, the evaluations of this section are only qualitative and may be uncertain by a factor of two or more in some cases. However, they do provide some guidance that was not available from the prior ENDF/B–V files which contain no reference to any of these processes.

A. (n,p) and (n;n′,p) Cross Sections.

The experimental database for this reaction seems to be limited to nine measurements, all near an incident–neutron energy of 14 MeV, as cited in Refs. 81–89. Three of these involve partial cross–section measurements of emitted–proton spectra using particle–detection methods. Those results are not too useful for the present purposes. In principal, it should be possible to determine the cross section by activation methods, measuring the residual activities of ^{115}Cd. However, ^{115}Cd has a metastable state ($11/2^-$, 173 keV, $t_{1/2}$=44.8 d), as well as a ground state ($1/2^+$), that will be populated by the (n,p) reaction. The cross section resulting in the activation of the ground state has been measured six times, with various results. Ignoring two exceptional values, the cross section seems to be 4–5 mb at approximately 14 MeV. A single measurement of the cross section for the excitation of the metastable state at 14.8 MeV gives a result of (7.7 ± 1.2) mb. Thus, the fragmentary experimental evidence suggests an (n,p) cross section of 10–15 mb at 14–15 MeV. The calculations indicate that the cross section is very largely due to pre–compound processes, and, near 14 MeV, the result calculated with ALICE was ≈ 14 mb, in reasonable agreement with the fragmentary experimental evidence. Thus, the evaluation uses the ALICE results to provide the (n,p) cross section. The same calculations were used to provide the evaluated (n;n′,p) cross sections and emission spectra. There is essentially no experimental evidence to test the result, and any activity measurement would not separate (n;n′,p) and (n,d) processes. Both processes have relatively small cross sections, ≈ 10 mb near 14 MeV and < 20 mb at 20 MeV, so the uncertainties in the evaluations are of little concern in most applications of the file.

B. (n,d) and (n;n′,d) Processes.

The available experimental information is confined to partial direct–detection results,[82] and is not sufficient to guide the evaluation of these two processes; therefore, the values from the statistical calculations are used. The results are very speculative, but the cross sections are ≈ < 20 μb, so the large uncertainties are not of much concern in most applications.

C. (n,t) and (n;n′,t) Processes.

These processes, and their treatment, are analogous to the (n,d) and (n;n′,d) reactions outlined above. The cross sections are even smaller than in the above case, and one measurement indicates a value of < 50 μb for the (n,t) cross section near 14 MeV.[90]

D. (n,^{3}He) and (n;n′,^{3}He) Processes.

Calculational estimates indicate that the cross sections for these processes are in the pb – μb region (a measurement[91] seems to set an upper limit at approximately this level), and, thus, the reactions were ignored in the evaluation.

E. (n,α) and (n;n′,α) Processes.

The ^{115}In(n,α) process results in ^{112}Ag which has a 3.14 h activity that can be reasonably measured. There have been at least seven such measurements,[83,92-97] all at incident–neutron energies of ≈ 14 MeV. With one exception, the results are closely grouped between ≈ 2.5–3.0 mb, with an average of 2.7 mb at 14.25 MeV. The measurements do not indicate the energy dependence of the cross section away from ≈ 14

MeV. Therefore, statistical calculations were used to guide the extrapolation over the full energy range. The results obtained with CADE and ALICE were reasonably consistent up to ≈ 16 MeV and differed by no more than a factor of two at 20 MeV. However, both calculated results were more than an order of magnitude smaller than the above-cited experimental values in the 14 MeV region. That is a disturbing discrepancy that may be due to pre-compound processes not included in these particular calculations. Hopefully, the calculated energy-dependent shape is qualitatively reasonable, and thus it was normalized to the experimental values near 14 MeV to give the (n,α) evaluation. The same normalization factor was used to obtain the (n;n',α) evaluation from the calculations. Certainly, these two evaluations, and the associated emission spectra, are very uncertain. However, the cross-section magnitudes do not exceed several mb below ≈ 16 MeV.

IX. PHOTON PRODUCTION PROCESSES

The photon-production data are made up of contributions from the (n,γ), (n;n',γ) to specific levels, and a continuum from all other photon-producing reactions.

Photon production for the (n,γ) reaction is dealt with by providing an energy-dependent photon multiplicity and spectra. The spectrum of photons from the neutron-capture reaction was taken from the work of Orphan et al.[98] at thermal energy. The average energy of the spectrum was determined and divided into the Q-value for the reaction in order to determine the low-energy photon multiplicity. The same spectrum was used at 20 MeV, with the multiplicity adjusted to conserve energy.

For photons associated with the inelastic scattering to specific levels, Warren's code CASCADE,[99] which incorporates the method used in Reffo's BRANCH code,[100] was used to obtain the energy-dependent cross sections for specific photons resulting from the de-excitation of the levels excited by the inelastic-scattering process.

For all other reactions, the photon production cross sections and spectra were calculated using the R-parameter formalism of Perkins et al.[101] The R-parameter formalism requires formal representation of energy distributions for all secondary particles (i.e., charged-particles as well as neutrons) in order to calculate the photon-production cross sections and spectra. Since the ENDF/B-VI formats and procedures allow for secondary charged-particle distributions in File 5 only if there is a single secondary particle, the file was translated to the ENDL format where energy distributions for all secondaries can be represented. The R(U) values used were taken from the "global" values of Ref. 101.

After entering the calculated photon-production data, energy conservation was calculated and verified to within 5% for all incident neutron energies.

X. THE ^{115}In(n,n')^{115m}In DOSIMETRY REACTION

Fast-neutron excitation of the first-excited isomeric level of ^{115}In (i.e., ^{115m}In) is a popular reaction for applications in neutron spectrum diagnostics (neutron dosimetry) for fast-fission reactors and other neutron environments. There are several reasons for its popularity: i) The cross section is large and it rises rapidly from a relatively low threshold. ii) The half life is very convenient for many applications. iii) The radioactive decay properties of ^{115m}In are amenable to precise measurements with relatively simple detector systems. iv) There exists an extensive experimental database for this reaction, which leads one to believe that the cross section ought to be relatively well–known over the energy range of interest for most contemporary applications. The latter point does raise certain questions: i) A careful inspection of this information indicates that there are some serious discrepancies in the differential database. ii) The current ENDF/B–V differential evaluation leads to C/E comparisons for integral data involving fission–neutron spectra which are sufficiently different from unity so that this reaction cannot be considered well enough known for precise dosimetry purposes.

The ENDF/B–V evaluation for this reaction is based on the work of Smith.[102] There are two significant shortcomings to this evaluation (beyond the above–mentioned integral/differential discrepancy) which indicate a need for revision: i) The data upon which it is based are quite old ($\leq$ 1975). Since that time an extensive collection of new differential information has accumulated. ii) The evaluation is derived from an eyeguide to the available differential data. Consequently, it is subjective and the uncertainty estimates provided are inadequate for contemporary applications (i.e., there does not exist a reliable covariance matrix for the evaluation).

The first step in the evaluation process was to review the status of the fundamental parameters which influence the measurement of this cross section by the activation method and, furthermore, determine how it will be applied in neutron dosimetry. Recent values for the pertinent parameters were obtained from the literature.[33,103,104] They are summarized in Table 2. A comparison with Ref. 103 shows that the accepted values for these parameters are essentially unchanged since 1976.

Table 2

Properties of indium and the ^{115}In(n,n′)^{115m}In reaction which are relevant to the present evaluation

Natural abundance:	^{113}In (4.3%) ^{115}In (95.7%)
Half life of ^{115m}In:	4.486 hours
Excitation energy for ^{115m}In:	0.336 MeV
Threshold for ^{115}In(n,n′)^{115m}In:	0.339 MeV
Decay modes for ^{115m}In:	IT 95.0% β 5.0%
Total internal conversion coefficient:	1.073
Number of 0.336 gamma–rays per decay of ^{115m}In :	0.459

The next step in the evaluation was to compile all the available differential data from the literature, as determined from CINDA[105] and CSISRS.[4] Furthermore, nuclear model calculations were performed with the code ABAREX[106] to determine the theoretical cross–section shape very close to threshold where the data are quite uncertain. The collected experimental values include the data previously considered in the 1976 evaluation by Smith,[102] as well as several new data sets. A total of 32 experimental data sets (147 data points) were included in the present evaluation.[57,58,107-141] Each data set was adjusted (wherever it was necessary and feasible) to insure consistency with the parameters from Table 2 and with contemporary neutron fluence standards (generally based on ENDF/B–V cross sections). This procedure was quite difficult to carry out, since the documentation was either poor, unavailable, or nonexistent for many of the data sets. The data were plotted and inspected for consistency. A number of data points were very inconsistent with the main body of information. However, none of the available differential data were rejected for this evaluation. It was often necessary to increase the errors substantially above the reported values, particularly for poorly documented and/or inconsistent points. Considerable subjectivity was involved in producing the needed estimates for these errors and their correlations. As an approximation, each of the data sets was treated as independent of the others, since those factors which lead to correlations between data sets (e.g., decay parameters) were generally quite well–known so that the correlated errors between sets were of minor concern.

The evaluation itself was carried out using the least–squares code GMA.[28] GMA requires an *a priori* estimate of the differential cross section in order to shift experimental values measured at arbitrary energies to the selected energy grid–point locations. The earlier evaluation of Smith[102] was used for this purpose at energies above 0.6 MeV. Near threshold, the results of the present ABAREX calculations, renormalized to match the evaluation of Smith at 0.6 MeV, were employed to establish the *a priori* set. The available data were rather sparse in certain energy regions (e.g,, above 15 MeV). Consequently, the *a priori* values were also introduced as fictitious data points, with relatively large errors, in order to provide stability to the GMA least–squares estimation procedure. This approach amounted to a mere convenience, with little impact on the evaluated results in energy regions where actual data were available. A fundamental problem was encountered in applying the least–squares estimation procedure of GMA in its existing form. The evaluated cross sections appeared to be systematically low across the entire energy range of the evaluation. It was decided that this unusual result was a manifestation of the phenomenon known as "Peelle's Puzzle".[142] GMA, in its original form, is set up so that the absolute errors used in computing data weighting factors are derived from the input data values. Consequently the low data values are more heavily weighted than higher values (even if the percent errors are the same). In fact, when correlations are present, it is possible for the evaluated values to fall below all the considered data points![143] This state of affairs was considered to be unacceptable, so it became necessary to revise GMA.[142] The approach taken was to employ the *a priori* estimate in computation of the data covariance matrix, using percent errors for the input uncertainties. This technique provided an evaluation that was much more consistent with the available experimental data. Iteration was required in the application of this method. Convergence toward the solution was rapid, so acceptable final results were obtained after just a few iterations. The final evaluated results are given in Tables 3 and 4. The chi–square per degree of freedom for the solution was 1.921, indicating a relatively modest degree of residual inconsistency in the experimental data. The final quoted errors for this evaluation were therefore obtained by multiplying the errors derived from GMA by the square root of this factor, namely, 1.386. These errors are $\leq$ 3% over much of the energy range of interest for dosimetry applications, which represents a vast improvement over ENDF/B–V.

Table 3

Evaluated cross sections and uncertainties for the $^{115}In(n,n')^{115m}In$ reaction

Energy (MeV)	Cross Section (mb)	Uncertainty (%)
0.350	0.5158	18.8
0.375	0.8953	27.9
0.400	1.531	10.6
0.450	2.259	6.7
0.500	3.086	6.7
0.550	4.192	6.7
0.600	6.262	8.6
0.650	12.92	4.6
0.700	17.21	5.4
0.800	28.50	3.7
0.900	49.36	4.5
1.000	68.16	3.1
1.100	78.91	3.6
1.200	110.5	2.4
2.000	268.3	2.4
2.250	324.8	2.6
2.600	346.2	2.4
3.500	334.6	2.3
4.250	314.1	2.4
6.000	348.6	2.8
6.250	347.6	3.8
7.500	317.4	3.3
8.500	306.1	3.6
10.000	260.7	3.8
13.100	87.48	4.4
14.000	62.49	3.3
15.000	57.98	2.7
16.000	56.04	7.9
18.000	54.40	8.4
20.000	54.79	11.8

Table 4

Uncertainty correlation matrix for the evaluated cross sections in Table 3

1000																			
14	1000																		
25	17	1000																	
43	22	70	1000																
44	22	68	139	1000															
37	23	78	111	107	1000														
35	18	47	108	113	73	1000													
57	33	108	174	173	171	127	1000												
51	28	88	156	157	138	120	210	1000											
70	38	128	219	220	204	165	304	261	1000										
56	33	100	171	172	159	132	238	206	296	1000									
77	46	144	232	232	228	176	336	285	413	335	1000								
63	42	127	183	179	201	130	282	233	342	282	407	1000							
88	59	172	251	248	273	188	389	324	477	404	590	527	1000						
89	60	173	254	252	275	192	394	329	483	412	601	538	809	1000					
84	57	164	240	238	260	180	373	310	456	387	563	503	754	776	1000				
90	61	175	257	255	278	195	400	332	489	416	609	541	817	840	783	1000			
91	61	178	261	259	283	196	405	337	496	422	615	550	826	850	792	856	1000		
88	59	173	252	250	274	189	392	325	478	403	589	522	782	800	747	810	825	1000	
73	52	135	196	194	213	152	310	250	371	306	457	394	597	603	569	624	616	605	1000
54	42	93	134	134	145	107	212	172	254	210	313	271	408	417	394	431	424	418	415
64	50	111	160	159	173	128	253	204	302	250	372	322	486	496	469	514	504	496	495
62	49	106	153	153	166	123	244	196	290	241	358	310	468	478	452	495	486	476	436
59	47	100	144	144	156	116	228	184	272	225	335	291	437	446	422	462	453	446	415
29	24	47	67	66	72	52	103	85	124	104	156	134	199	202	195	207	211	208	187
20	16	34	48	48	52	38	75	61	90	75	111	96	144	146	140	151	151	150	147
22	18	37	53	53	57	42	83	68	99	83	123	107	159	162	155	166	167	166	160
19	15	32	45	45	49	35	70	58	84	71	108	92	137	139	135	141	147	144	121
19	15	32	46	45	49	35	71	59	85	72	109	93	138	140	137	142	148	145	122
16	14	26	37	37	40	29	57	48	69	58	87	75	111	113	110	115	119	116	98

1000									
388	1000								
327	385	1000							
321	376	351	1000						
159	168	160	154	1000					
130	141	126	131	259	1000				
142	153	137	142	279	472	1000			
99	101	102	91	138	81	98	1000		
100	101	103	91	131	71	86	149	1000	
80	82	83	74	90	43	53	81	82	1000

The evaluated results are also plotted in Figs. 8 and 9. Figure 10 shows the error correlations in terms of a three–dimensional histogram. This figure corresponds to the values from Table 4.

Comparison is made between ENDF/B–V and the experimental data. The present evaluated cross sections tend to be a few percent larger than corresponding values from the earlier evaluation of Smith.[102] It is of interest to compare the results of the present evaluation with the available integral data for a standard fission spectrum. The integral value for the ^{252}Cf spontaneous fission neutron spectrum was used for this purpose. Mannhart has evaluated the available experimental integral data, and he obtained the result 197.6 mb (±1.4%).[144] Mannhart has also provided an evaluation of the neutron spectrum.[144] Therefore, it was possible to calculate the integral value from differential information. The result is 189.6 mb (±2.2%). This leads to C/E = 0.960. The difference of 4.0% is a bit beyond the range of the errors but, in general, the agreement is pretty good. In this respect, the present evaluation also represents a significant improvement over the ENDF/B–V result based on the work of Smith.[102]

Owing to ENDF format considerations, this particular evaluation cannot be included in the general purpose file for elemental indium. Consequently, it has been placed in a special–purpose file explicitly intended for dosimetry purposes.

XI. SUMMARY REMARKS

The above discussion documents a comprehensive evaluated neutronic file for elemental indium suitable for the large majority of applications. This file differs from the prior ENDF/B–V indium files in major ways, including the provision of contributions of major neutron–induced reactions which were not in the previous files. Uncertainty information is provided to a good degree, making possible sensitivity assessment. An ancillary file deals with the ^{115}In(n,n′)^{115m}In reaction, widely used for dosimetry purposes. This new dosimetry file is an improvement on the prior ENDF/B–V version, particularly including detailed uncertainty specification and providing a better consistency with integral bench–mark measurements.

Significant improvement of the present evaluations will require new measurements, in particular:

1. Energy–average total cross section measurements with emphasis on the 1 keV to 1 MeV and 10 to 20 MeV regions. Such measurements are straightforward, but must be done with care if the desired ≈ 1% accuracy is to be achieved.

2. At present there is no experimental knowledge of elastic scattering above ≈ 15 MeV. The lack is serious in the determination of the non–elastic cross section. A few good elastic–scattering angular distributions should be measured between 10 and 20 MeV. Accuracies should generally be 5% or better, with 50 or more differential values distributed between 10° to 160°. Such measurements are difficult, but possible.

3. At the present time, (n,2n′) cross sections must be largely construed from activation measurements of isomer cross sections. It is desirable that a systematic

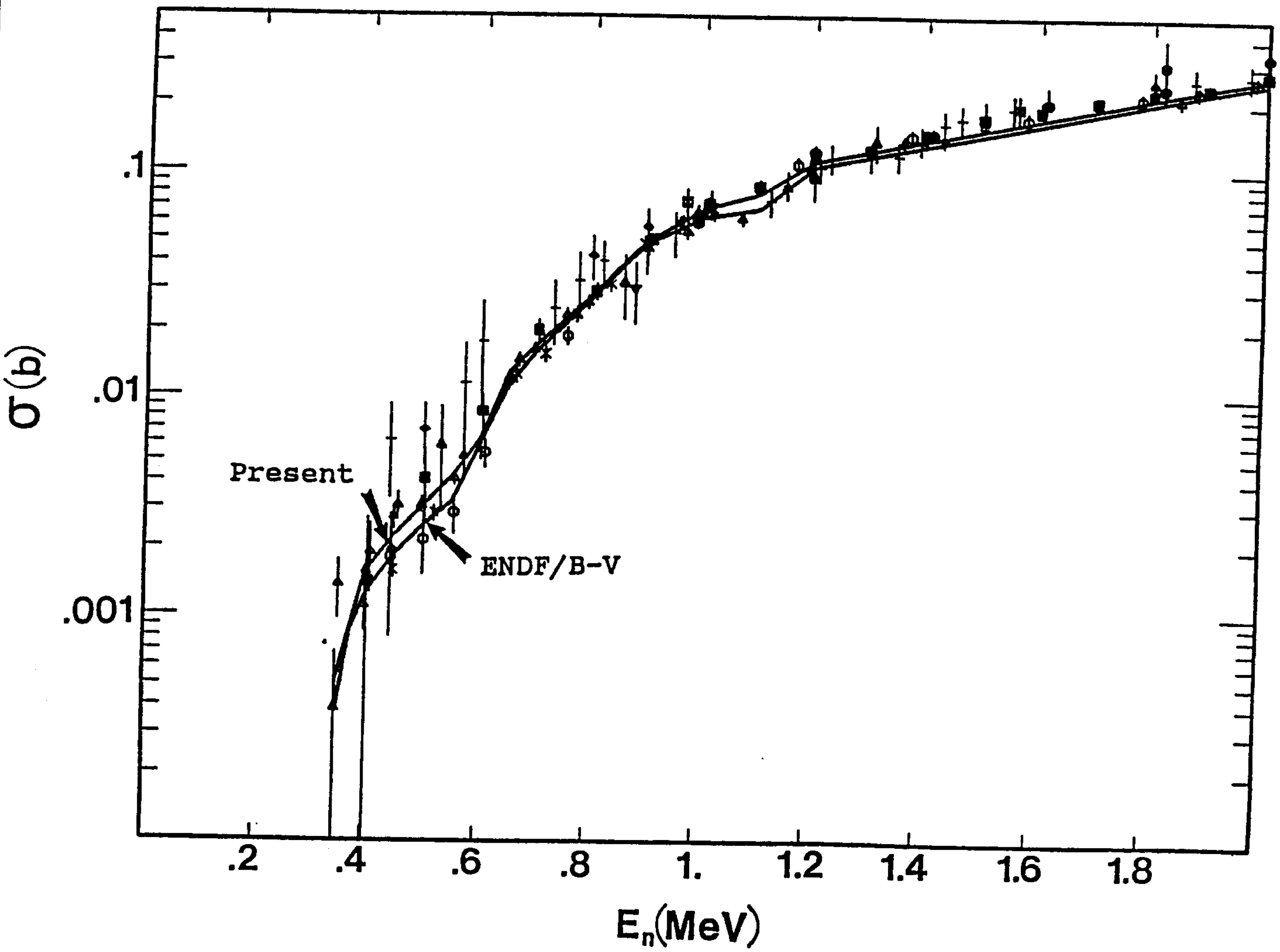

Fig. 8. Semi–log plot of experimental and evaluated cross sections for $^{115}In(n,n')^{115m}In$. Only the region below 2 MeV is shown; "A" indicates the present evaluation, and "B" that of ENDF/B–V.

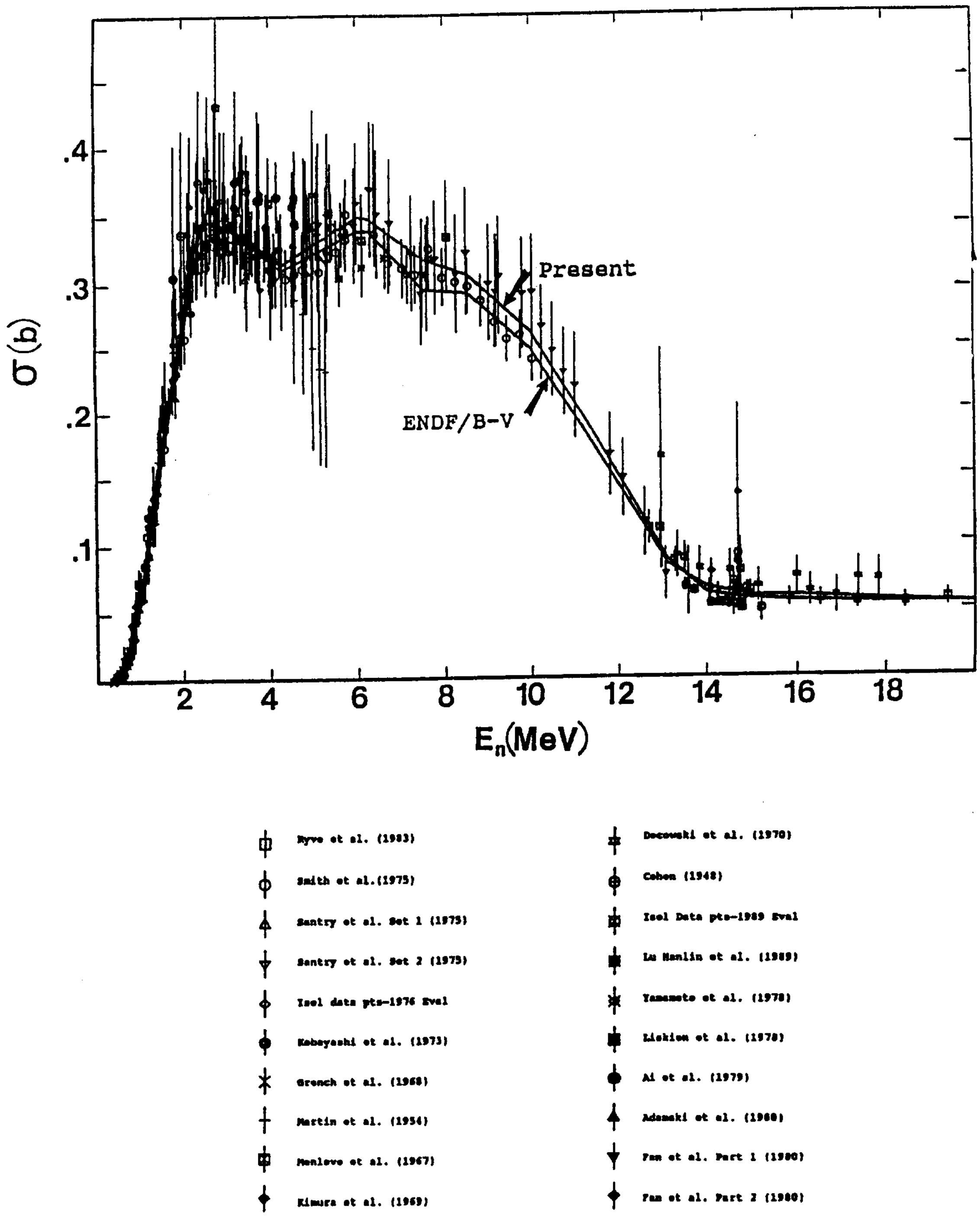

Fig. 9. Linear plot of experimental and evaluated cross sections for $^{115}In(n,n')^{115m}In$. The entire region from 0 to 20 MeV is shown; "A" indicates the present evaluation, "B" that of ENDF/B–V.

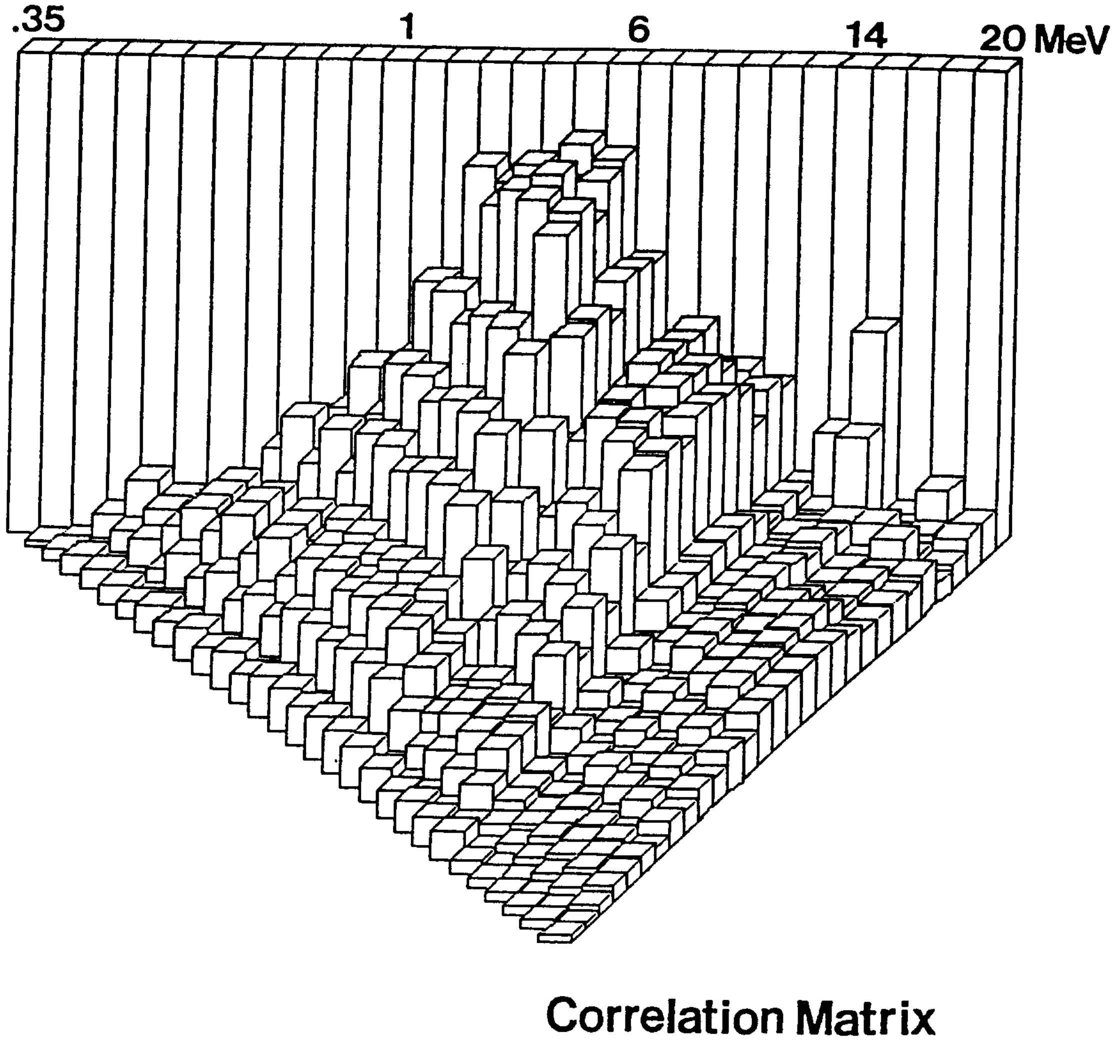

Fig. 10. Three–dimensional histogram of the uncertainty correlations provided in Table 4.

(n,2n′) study be made using prompt–detection methods (e.g., scintillation tank). Such measurements are feasible.

4. The (n,γ) cross section is large and relatively uncertain and/or discrepant, particularly above 100 keV. Careful measurements are necessary before the (n,γ) situation can be significantly improved. They are technically feasible.

Finally, certain aspects of nuclear models for the interaction of fast neutrons with nuclei in the mass range of indium have been very carefully studied (e.g., the dispersive optical model). The calculational tools to apply these improved physical concepts to the provision of evaluated data in a wide scope are not sufficiently well developed.

REFERENCES

1. Evaluated Nuclear Data File–B (ENDF/B), National Nuclear Data Center, Brookhaven National Laboratory. Throughout this document the term ENDF/B is used to reference this file without further citation. The various versions are designated as, for example, ENDF/B–V (version five) and ENDF/B–VI (version six).

2. S. Mughabghab, M. Divadeenam, and N. Holden, Neutron Cross Section Vol.–1, Part–A, Academic Press Inc, New York (1984); also, S. Mughabghab and C. Dunford, private communication (1982).

3. D. Cullen, Lawrence Livermore National Laboratory Report, UCRL–50400, Vol–17, Part–C (1979); also, D. Cullen, private communication (1989).

4. National Nuclear Data Center, Brookhaven National Laboratory.

5. D. Foster and D. Glasgow, Phys. Rev. C3 576 (1971), Sys.=2%.

6. T. Divadeenam, Dissertation Abstracts, Section B, 28 3834 (1967); data abandoned, as it was very low.

7. J. Coon, E. Graves and H. Barschall, Phys. Rev. 88 562 (1952), Sys.=2%.

8. J. Peterson, A. Bratenahl and J. Stoering, Phys. Rev. 120 521 (1960), Sys.=2%.

9. A. Bratenahl, J. Peterson and J. Stoering, Phys. Rev. 110 217 (1958), Sys.=4%.

10. D. Kent, S, Puri, S. Snowdon and W. Bucher, Phys. Rev. 125 331 (1962), Sys.=4%.

11. D. Miller, R. Adair, C. Bockelman and S. Darden, Phys. Rev. 88 83 (1952); abandoned due to large scatter.

12. A. Jain, R. Chrien, J. Moore and H. Palevsky, Phys. Rev. B137 83 (1965); abandoned, low in magnitude and at very low energies.

13. C. Bockleman, R. Peterson, R. Adair and H. Barschall, Phys. Rev. 76 277 (1949); abandoned due to large scatter.

14. P. Malmberg and S. Snowdon, Phys. Rev. 128 351 (1962), Sys.=4%.

15. R. Tabony and K. Seth, Ann. Phys. 46 401 (1968); abandoned, much too low.

16. W. Poenitz and J. Whalen, Argonne National Laboratory Report ANL/NDM–80 (1983), Set–1, Sys.=4%.

17. W. Poenitz and J. Whalen, Argonne National Laboratory Report ANL/NDM–80 (1983), Set–2, Sys.=3%.

18. W. Poenitz and J. Whalen, Argonne National Laboratory Report ANL/NDM–80 (1983), Set–3, Sys.=2%.

19. A. Smith, P. Guenther and J. Whalen, Nucl. Phys. A415 1 (1984), Sys.=2%.

20. W. McGarry, J. Elliot and W. Faust, Report NRL–4666 (1955); abandoned, unduly low.

21. F. Manero, Nucl. Phys. 65 419 (1965), Sys.=2%.

22. W. Dilg and H. Vonach, Report EANDC(E)–150, 40 (1972); abandoned, too low in energy.

23. V. Giordano, C. Manduchi, M. Russo–Manduchi and G. Segato, Nucl. Phys. A302 83 (1978), Sys.=4%.

24. P. Egelstaff, private communication (1954), Sys.=4%.

25 Ju. Dukarevich, A Djumin and D. Kaminker, Nucl. Phys. A92 433 (1967), Sys.=2%.

26. V. Vladimirski, I. Radkewich and W. Sokolowsky, 1955 Geneva Conf. 4 22 (1955); abandoned, large scatter.

27. G. Gorlov, N. Lebedeva and V. Morozov, Yandernay Fizika 6 910 (1967); abandoned, abnormally low point.

28. W. P. Poenitz, Brookhaven National Laboratory Report, BNL–NCS–51363 (1981).

29. A. Smith, P. Guenther, J. Whalen, I. Van Heerden and W. McMurray, J. Phys. G11 125 (1985).

30. A. Smith, S. Chiba, P. Guenther and R. Lawson, to be published.

31. G. Wick, Atti R. Accad. Ital. Memorie, 13 1203 (1943).

32. A. Gilbert and A. Cameron, Can. J. Phys. 43 1446 (1965).

33. C. Lederer and V. Shirley, eds., Table of Isotopes 7th Edition, John Wiley and Sons, New York (1978).

34. P. Guenther, Report to the IAEA Coordinated Research Program on the Measurement and Analysis of Double–Differential Neutron–Emission Spectra in (p,n) and (α,n) Reactions (1989).

35. M. Blann, Lawrence Livermore National Laboratory Report, UCID–20169 (1984).

36. D. Wilmore, Harwell Report, AERE–R–11515 (1984).

37. P. Bracazio and A. Cameron, Can. J. Phys. 47 1029 (1969).

38. P. Guenther et al., Argonne National Laboratory Report, ANL/NDM–107 (1988).

39. R. Block et al., Proc. Conf. on New Developments in Reactor Physics and Shielding, Conf. 720901 2 1107 (1972).

40. J. Gibbons et al., Phys. Rev. 122 186 (1961).

41. B. Diven et al., Phys. Rev. 120 556 (1960).

42. H. Schmitt and C. Cook, Nucl. Phys. 20 202 (1960).

43. R. Block et al., Proc. Conf. on Nuclear Data, Saclay 203 (1961).

44. E. Haddad et al., General Atomics Report, GA–3874 (1963).

45. W. Poenitz, Argonne National Laboratory Report, ANL–83–4–239 (1982).

46. J. Hellstroem, J. Nucl. Energy 27 71 (1973).

47. D. Kompe, Nucl. Phys. A133 513 (1969).

48. W. Poenitz, NEA Report, EANDC(E)–66 (1966).

49. M. Budmar et al., IAEA Report, INDC(YUG)–6 (1979).

50. V. Koroleva and Ju. Ja Stavisskij, Atom Energy 20 431 (1966).

51. Ju. Popov and F. Shapiro, J. Exp. Theo. Physics 42 988 (1962).

52. L. Spitz et al., Nucl. Phys. A121 655 (1968).

53. P. Moldauer, private communication (1982).

54. R. Barrall, J. Homes and M. Silbergeld, Airforce Laboratory Report, AFWL–TR–68 134 (1976).

55. J. Temperley and D. Barnes, Ballistic Research Laboratory Report, BRL–1491 (1970).

56. G. Salaita and D. Eapen, Trans. Am. Nucl. Soc., ANS 16 59 (1970).

57. D. Santry and J. Butler, Can. J. Phys. 45 757 (1976).

58. H. Menlove, K. Coop, H. Grench and R. Sher, Phys. Rev. 163 1308 (1967).

59. W. Ashby et al., Proc. Conf. on Peaceful Uses of Atomic Energy, Geneva 15 2494 (1958).

60. R. Prestwood and B. Bayhurst, Phys. Rev. 121 1438 (1961).

61. H. Rortser, Nucl. Phys. A109 694 (1968).

62. W. Nagel, J. Nucl. Energy 20 475 (1966).

63. A. Paulsen, H. Liskien and R. Widera, Atomkernenergie 26 34 (1975).

64. B. Minetti and A. Pasquarelli, Z. Phys. 217 83 (1968).

65. G. Curzio and P. Sona, Nuovo Cimento B54 319 (1968).

66. K. Kayashima, A. Nagao and I. Kumabe, NEA Report, NEANDC(J)–61U 94 (1979).

67. M. Borman et al., NEA Report, EANDC(E)–76 51 (1967).

68. P. Francois and N. Shakir, J. Inorg. Nucl. Chem. 41 1212 (1979).

69. T. Ryves et al., J. Phys. G9 1549 (1983).

70. R. Prasad and D. Sarkar, Nucl. Phys. A94 476 (1967).

71. P. Decowski et al., Nucl. Phys. A204 121 (1973).

72. J. Araminowicz and J. Dressler, Inst. Badan Jadrowych Report, INR–1464 14 (1973).

73. J. Janczyszyn and L. Gorski, J. Radio. Analy. Chem. 14 201 (1973).

74. E. Holub and N. Cindro, J.Phys. G2 405 (1976).

75. K. Garg and C. Khurana, Indian J. Pure and Applied Phys. 17 525 (1979).

76. A. Chatterjee et al., Trombay Report Series, BARC–474 50 (1970).

77. A. Reggoug et al., data available at the NNDC.

78. Li Jianwei et al., Chinese J. Nucl. Phys. 10 52 (1988).

79. H. Liskien, Nucl. Phys. A118 379 (1968).

80. R. Howerton, Tabulation of Q–values, informal LLNL report.

81. V. Verbinski et al., Phys. Rev. 108 779 (1957).

82. R. Peck, Phys. Rev. 123 1738 (1961).

83. V. Levkovski et al., Yadernaya Fizika 10 44 (1969).

84. K. Kayashima et al., NEANDC(J)–61U 94 (1979).

85. R. Coleman et al., Proc. Phys. Soc. 73 215 (1959).

86. T. Ryves et al., J. Phys. G9 1549 (1983).

87. J. Temperley and D. Barnes, Ballistic Research Lab. Report, BRL–149 (1970).

88. T. Mavaddat et al., J. Inorg. Nucl. Chem. 36 953 (1974).

89. D. Allan, Nucl. Phys. 24 274 (1961).

90. S. Qaim, Nucl. Phys. A438 384 (1985).

91. S. Qaim, J. Inorg. and Nucl. Chem. 36 239 (1974)

92. J. Temperley and D. Barnes, as per Ref. 87.

93. H. Blosser et al., Phys. Rev. 100 429 (1955).

94. T. Nagel, J. Nucl. Energy, 20 475 (1966).

95. R. Coleman et al., Proc. Phys. Soc. 73 215 (1959).

96. T. Ryves et al., J. Phys. G9 1549 (1983).

97. B. Sen, Nucl Phys. 38 601 (1962).

98. V. Orphan, N. Rasmussen and T. Harper, Gulf General Atomic Report, GA–10248/DASA 2570 (1970).

99. W. Warren, R. Howerton and G. Reffo, CASCADE – CRAY program for gamma production from discrete–level inelastic scattering, Lawrence Livermore National Laboratory Internal Report, PD–134 (1986).

100. G. Reffo, IDA – A modular system of nuclear model codes for the calculation of cross sections for nuclear reactors, Centro Ricerche Energia, Bologna (1980), unpublished.

101. S. Perkins, R. Haight and R. Howerton, Nucl. Sci. and Eng. 57 1 (1975).

102. D. Smith, Argonne National Laboratory Report, ANL/NDM–26 (1976).

103. J. Tuli, "Nuclear Wallet Cards", National Nuclear Data Center, Brookhaven National Laboratory (1985).

104. J. Blachot and G. Marguier, Nuclear Data Sheets 52, 565 (1987).

105. CINDA, "An Index to the Literature on Microscopic Neutron Data", International Atomic Energy Agency, Vienna (1935–89).

106. ABAREX, "A Spherical Optical Model Code", P. Moldauer, private communication (1983), and as revised by R.D. Lawson (1986).

107. D. Smith and J. Meadows, Argonne National Laboratory Report, ANL/NDM–14 (1975).

108. D. Smith and J. Meadows, Nucl. Sci. Eng. 60, 319 (1976).

109. R. Barrall, J. Holmes and M. Silbergard, U. S. Airforce Report, AFWL–TR–68–134 (1969).

110. R. Barrall, M. Silbergard and D. Garner, Nucl. Phys. A138, 387 (1969).

111. J. Temperley and D. Barnes, as per Ref. 87.

112. H. Roetzer, Nucl. Phys. A109, 694 (1968).

113. H. Roetzer, Oesterr. Akad. Wiss., Math–Naturw. K, Sitzungsber 76, 289 (1968).

114. I. Heertje, W. Nagel and A.H.W. Aten, Jr., Physica 30, 775 (1964).

115. W. Negel and A.H.W. Aten, Jr., Physica 31, 1091 (1965).

116. A. Pazsit and J. Csikai, Sov. J. Nucl. Phys. 15, 232 (1972).

117. B. Minetti and A. Pasquarelli, Z. Physik 217, 83 (1968).

118. K. Kobayashi, I. Kimura, H. Gotoh and H. Yagi, J. Nucl. Energy 27, 741 (1973).

119. H. Grench and H. Menlove, Phys. Rev. 165, 1298 (1968).

120. A. Ebel and C. Goodman, Phys. Rev. 93, 197 (1954).

121. H. Martin, B. Diven and R. Taschek, Phys. Rev. 93, 199 (1954).

122. I. Kimura, K. Kobayashi and T. Shibata, J. Nucl. Sci. Tech. (Japan) 6, 485 (1969).

123. P. Decowski, W. Grochulski, A. Marcinkowski, J. Karoly, J. Piotrowski, E. Saad, K. Siwek–Wilczynska, I.M. Turckiewicz and A. Wilhelmi, Inst. Badan Jadrowych Report, INR–1197 (1970).

124. S. Cohen, Nature 161, 475 (1948).

125. P. Bornemisza–Pauspertl, J. Karolyi and G. Peto, Atomyi Koezlemenyek 10, No. 2, 112 (1968).

126. Lu Hanlin, Ke Wai, Zhao Wenrong, Yu Weixiang and Yuan Xialia, Institute of Atomic Energy, Beijing, private communication (1989).

127. S. Yamamoto, K. Kobayashi, S.A. Hayashi and I. Kimura, Annual Report of the Research Reactor Institute, Kyoto Univ., Vol. 11, 121 (1978).

128. H. Liskien, F. Arnotte, R. Widera and A. Paulsen, Nucl. Sci. and Eng. 67, 334 (1978).

129. T. Ryves, Ma Hongchang, S. Judge and P. Kolkowski, J. Phys. G 9, 1549 (1983).

130. C. Hudson and W. Alford, Bull. Am. Phys. Soc. 21, 188 (1976).

131. G. Magnusson and I. Bergqvist, Nucl. Technol. 34, 114 (1977).

132. P. Anderson, S. Lundberg and G. Magnusson, Lund Univ. Report LUNF–DG–3021 (1978).

133. C.–F. Ai and J.–C. Chou, J. of Nucl. Sci. (Taiwan) 16, No. 3, 157 (1979).

134. L. Adamski, M. Herman and A. Marcinkowski, Ann. Nucl. Energy 7, No. 7, 397 (1980).

135. Fan Pei–Guo, Lu Hanlin, Li Ji–Zhou and Huang Jian–Zho, Chinese Nuclear Physics 2, No. 4, 337 (1980).

136. I. Garlea, Cr. Miron, D. Dobrea, C. Roth, T. Musat and H.N. Rosu, IAEA Report INDC(ROM)–15 (1983).

137. K. Kudo et al., NEA Prog. Report NEANDC(J)–106/J, p. 1 (1984).

138. V. Demekhin, B. Leshchenko, V. Majdanjuk and G. Peto, Proc. 1983 Kiev Conf. 3, 195 (1983).

139. A. Reggoug, G. Paic and A. Chiandli, Nucl. Instr. and Meth. 227, 249 (1984).

140. K. Kobayashi and I. Kimura, Proc. Conf. Nuclear Data for Science and Technology, ed. S. Igarasi, Saikon Publishing Co., Tokyo, p. 261 (1988).

141. R. Pepelnik et al., NEA Prog. Report NEANDC(E)–262U, p. 32 (1985).

142. S. Chiba and D. Smith, to be published as an Argonne National Laboratory Report, ANL/NDM–116 (1990).

143. F. Perey, Proc. International Conf. on Neutron Physics and Nuclear Data for Reactors, Harwell, United Kingdom, p. 104 (1978).

144. W. Mannhart, Reactor Dosimetry: Methods, Applications and Standardization, eds. H. Farrar IV and E. Lippincott, ASTM STP–1001, Amer. Soc. for Testing and Materials, Philadelphia, p. 340 (1989).